University of Edinburgh
College of Science and Engineering
School of Physics
MSc in Acoustics and Music Technology
Final Research Project: Dissertation

Voice coil temperature in loudspeaker performance:
Causes, effects and prevention techniques

Adam J. Hill
s0787532

I, Adam J. Hill, confirm that this dissertation and the work presented in it are my own achievement.

1. Where I have consulted the published work of others this is always clearly attributed.
2. Where I have quoted from the work of others the source is always given. With the exception of such quotations the dissertation is entirely my own work.
3. I have acknowledged all main sources of help.
4. If my research follows on from previous work or is part of a larger collaborative research project I have made clear exactly what I have contributed myself.
5. I have read and understood the penalties associated with plagiarism.

Signed:

Matriculation Number: s0787532

Date: August 21, 2008

Abstract

The modern day loudspeaker's performance is limited by a number of factors. An important limiting factor is voice coil heating. Most loudspeakers are extremely inefficient. That is, of the input electrical power only a small fraction of that power is actually converted into acoustical power. The vast majority of this lost power is converted into heat in the voice coil. The heat generated can lead to a significant loss of performance and may eventually lead to the destruction of a loudspeaker. It is important to understand the causes and effects of voice coil temperature gain to allow for loudspeakers that are designed in anticipation of this problem. This paper will explore the principles behind loudspeaker behavior and the simulation of and experimentation on a loudspeaker under varying voice coil temperatures. This will help to understand exactly how the voice coil's temperature affects the overall loudspeaker performance.

Table of Contents

Acknowledgements

This project would not have been possible without the guidance and supervision of Dr. Jonathan Kemp. His expertise in acoustical measurements is what made this project feasible in the limited amount of time given. Also, I would like to thank my director of studies, Professor Murray Campbell, for his support and encouragement and also Mr. Les Russell for his assistance with my experimental setups.

It is also necessary to acknowledge my former academic advisor at Miami University, Dr. Jade Morton. Dr. Morton encouraged me to not restrict my graduate program search to the United States, but to also look internationally. Without her guidance, I would have never ended up in Edinburgh.

Finally, I would not have been able to study in the Acoustics & Music Technology MSc program at the University of Edinburgh without the endless support from my loving family back in Chicago. They have helped me in every way that they can to pursue an education in a field that I have come to love. Without them I would have never been able to take part in this great program.

1. Introduction

Loudspeaker performance optimization has been the subject of numerous research projects for the better part of a century. These projects have focused on everything from the materials used for the voice coil and diaphragm to the volume of enclosed air in the speaker. One area that has been explored, although maybe not to as great of an extent as the other areas, is the effect of voice coil temperature on loudspeaker performance.

Ideally, a loudspeaker would operate in a linear manner. A linear increase of input power would directly correspond to a linear increase of output power. Unfortunately, this is not possible under all realistic (or unrealistic) operating conditions. Nonlinearities can arise due to everything from an overdriven signal to impedance mismatches and of course due to voice coil heating.

The question is exactly how much does voice coil heating play into the occurrence of this non-linear behavior? Is it a negligible factor or can it seriously degrade the output's audio quality? Also, could this voice coil heating cause permanent damage to the loudspeaker?

These questions, among others, will be addressed in this paper using the knowledge of previous work done in this area as well as original experimental work through the use of logarithmic sinusoidal sweeps and Maximum Length Sequences (MLS). The experimental work will measure the response of a loudspeaker at various on-axis and off-axis positions as its voice coil heats up.

As well as referencing previous work and original experimental work, a simple loudspeaker performance simulator will be developed to give a basic idea of how different performance parameters can vary depending on voice coil temperature. This could help to explain the change in measured performance during experimentation.

Chapter 2 will outline the project goals and specifications. This will include the research, simulation and experimentation goals. Chapter 3 will give a brief summary of existing work and knowledge concerning voice coil temperature effects and prevention methods. Chapter 4 will cover loudspeaker principles. This will include a brief history of the loudspeaker, the

structural details of a general cone driver, the electrical/mechanical/acoustical relationship of the loudspeaker parameters, the common methods of performance evaluation, the known effects of voice coil heating and the methods to minimize voice coil heating.

Chapter 5 will present a simple loudspeaker simulation using original MATLAB software. This will cover the simulation methods including the key parameters and equations and will also describe the methods of software implementation.

Chapter 6 will discuss the loudspeaker experimentation. It will go over the experimental setup, the measurement techniques and the original MATLAB software written to carry out these experiments. Chapter 7 will present the experimental results including a detailed analysis.

The paper will be concluded in Chapter 8 directly followed by a reference section. A quick software user's guide will be presented in Appendix A. All MATLAB code and key measurement data/plots are contained on the CD that is included with this paper.

2. Project goals and specifications

The main aim of this project it to gain a thorough understanding of the effects of voice coil temperature on loudspeaker performance. The gained knowledge of temperature effects will aide my future exploration of the field of loudspeaker design and audio engineering. Work will be divided into three separate areas:

1) Research of loudspeaker principles
2) Simulation of loudspeaker performance with varying design parameters
3) Measurement of loudspeaker behavior under varying voice coil temperature levels

2.1 Research goals

Loudspeaker design has become a very complex field with numerous known parameters that can have great effect on loudspeaker performance. There has been a great deal of research performed in this area and it is very important to study at least the most commonly accepted loudspeaker design principles. Without this knowledge it would be impossible to accurately analyze the experimental results. The primary research topics will be:

1) Loudspeaker structural details
2) Electrical/Mechanical/Acoustical relationship of design parameters
3) Performance evaluation techniques
4) Known effects of voice coil temperature
5) Solutions to limit voice coil temperature increase

2.2 Simulation goals

The simulation will not be the focus of this project. Its purpose will be to give a simple illustration of how a chosen design or operational parameter can affect various aspects of a loudspeaker's performance. The simulation should allow a user to enter a loudspeaker's Thiele-Small parameters to get a performance prediction. Once experimental results are collected and processed, the simulation can serve as a tool to illustrate exactly how the voice coil temperature affected the loudspeaker's performance.

2.3 Experimentation goals

This project will focus on experimentation. The primary goal of all experiments will be to determine the loudspeaker's frequency and impulse response at a given listening position with a known voice coil temperature. The two measurement techniques will be logarithmic sinusoidal sweeps and Maximum Length Sequences (MLS). Both methods are commonly used for acoustical measurements and should, if performed correctly, give results that are in agreement. This should help ensure the reliability of the experimental results and will help develop the conclusions to this research project.

3. Existing work/knowledge

The effects of voice coil heating have been the focus of a number of research projects. These projects have included exploring techniques for voice coil temperature estimation [5] [6]. These projects were aimed at determining the voice coil temperature without any direct measurements other than knowledge of the input signal characteristics and the thermal time constants of the drivers used. This system was used to apply negative impedance to the system to counteract the voice coil impedance increase with temperature. Similar studies have been carried out focusing on amplifier design [12] [13]. These projects have taken the knowledge of the thermal properties of the voice coil and have designed amplifier circuitry to that works to reduce the effects of voice coil heating.

The majority of voice coil heating research has focused on developing techniques to counteract the increased voice coil resistance. Fewer projects have focused on specifically studying the effects on the frequency response of the driver at various measurement orientations. It is known that the acoustical output should decrease as the voice coil temperature rises [2], but is this decrease linear over the entire frequency range and is it constant from on-axis to off-axis positions? These topics will be explored in this project.

4. Loudspeaker principles

Loudspeaker devices can also be referred to as transducers or drivers. In this paper, the radiating device will be referred to as the driver. The overall enclosure (including the driver) will be referred to as the loudspeaker. This research project focuses on the dynamic cone driver mounted in a sealed enclosure. The driver/sealed enclosure loudspeaker system is the simplest of all loudspeaker systems (and also fairly common). Adding ports and/or horns to the system adds to its complexity and requires many more considerations in regard to design and simulation. The simplicity of the sealed enclosure will allow this research to target temperature effects without worrying about additional parameter contributions to the performance of the loudspeaker.

4.1 Brief history

The dynamic cone driver has seen only minor improvements to its design since it was first conceptualized by Siemens in 1874 and brought into its modern form by Rice and Kellogg in 1925 [1]. Since then the basic principles have remained unchanged. Improvements include the usage of better materials in the driver and enclosure construction. More attention is now paid to the interaction between all the components' parameters in a loudspeaker thanks to the work of Thiele, Small and Benson [11]. This work created what is now known as the Thiele-Small parameters. This set of parameters allows for manufacturers to advertise the specifications of their drivers to best help engineers create loudspeakers with maximized performance characteristics. These parameters will be discussed in more detail in Chapter 4.4.

Image 4.1: 1920's loudspeakers [18]

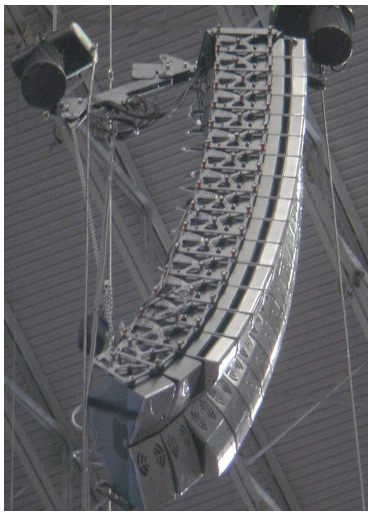

Image 4.2: Modern day PA

4.2 Structural details

There are five separate elements in the moving system of a driver: the cone, the outer suspension (surround), the inner suspension (spider), the voice coil and the dust dome (**Figure 4.3**) [1]. These five elements must work well together or else various forms of distortion can arise.

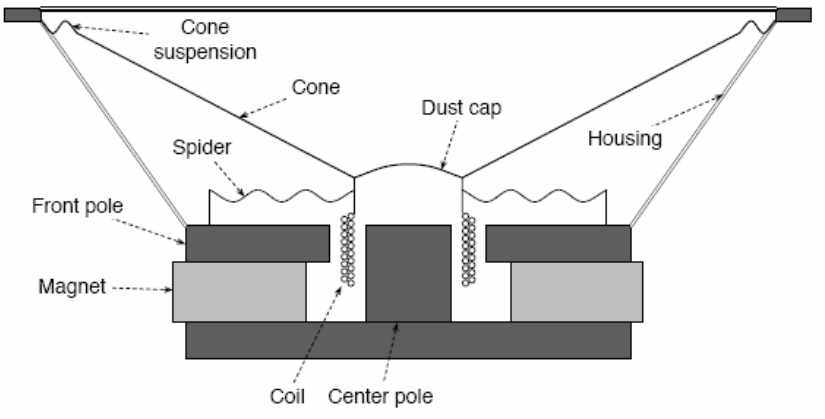

Figure 4.3: Loudspeaker elements (not to scale) [6]

The cone is the part of the driver that radiates the sound. It is important to make the cone out of a material that is rigid enough to hold together under heavy drive situations but also be able to provide high damping to avoid the reflection of waves along with cone's surface [1]. It is important to understand that the cone does not move forward and backward in complete unison; the cone actually moves in a quick ripple, going from the inner portion of the cone which is nearest to the voice coil outwards to the surround. Since the outer part of the cone doesn't move at exactly the same moment as the inner part, an outward moving wave is created. When this wave reaches the surround it can be partially reflected back towards the inner part of the cone due to a lack of damping in the cone and surround [1].

This can be easily related to the problem of voltage reflection in electronics. Ideally, two components will be connected that have equal input/output impedances. This allows for 100% of the voltage sent from one source to be received by the other. With an impedance mismatch, there will be a certain percentage of the voltage reflected back to the source which will interfere with the forward traveling voltage, possibly causing the system to behave other than expected. This is the same with the waves in the cone. These reflected waves can interact with the forward going waves and cause the driver to break up (distort). An

additional effect can be a variable radiating surface area on the cone [2]. This causes emphasis to be placed on the material used to construct the cone.

The two parts of the suspension system, the surround (outer) and spider (inner), add stability to the driver. The surround attaches the outer part of the cone to the driver's metal frame. Along with providing stability for the cone, the surround also contributes to the damping of the waves traveling along the cone. The stiffness of the surround adds to the mechanical resistance of the driver, but is necessary to have a certain amount of stiffness to keep the cone centered [1].

The spider is usually folded like an accordion and attaches the voice coil former (cylindrical object which the voice coil wraps around) to the metal frame of the driver. The spider serves as a stabilizer for the voice coil, making sure it remains centered in the magnetic air gap inside the driver. While the spider is very stiff in the direction perpendicular to the coil's movement, it is fairly flexible in the direction parallel to the coil motion [1]. If the spider isn't stiff enough in the perpendicular direction, the voice coil could begin to rub against the pole pieces causing the driver to distort and possibly destroy itself. A double spider configuration is commonly used in low frequency drivers to increase stability [1]. The spider also contributes to the driver's resonant frequency when operating at high drive levels and in some deigns must be constructed of a porous material to allow for the venting of enclosed air around the voice coil [1].

The voice coil is a cylindrical coil of tightly wound copper or aluminum wire that is located in the magnetic air gap in a driver. The electrical current moving through a wire will induce a magnetic force field surrounding the wire. Since the voice coil is sitting in the magnetic field of the driver's magnet, when a current is applied to the coil the added magnetic force field will naturally try to move towards magnetic stability (positive to negative, negative to positive) which in turn causes the driver to move [1]. The voice coil is where the vast majority of the heat is generated due to inefficiencies during the conversion from electrical to mechanical energy [2].

There are a number of design parameters that can either increase or decrease the amount of heat generated in the voice coil. One parameter is the voice coil's diameter (of its cylindrical former). When this diameter is increased (with the DC resistance and conductor length

remaining the same), the cross-sectional area of the conductor is increased. This decreases the resistance per unit length (current can flow more easily through the wire). The decrease in resistance per unit area will result in less heat buildup, allowing the voice coil to operate cooler [8].

Also, the height of the cylindrical structure of the voice coil affects the heat generated in the same way. This is especially useful if the driver design calls for the voice coil to overhang the magnetic air gap [8]. This means that the coil will be taller than the magnetic air gap so that there is always an equal length of conductor in the gap. The added height to the voice coil (with the conductor length and DC resistance remaining the same) requires a decrease in the wire gauge resulting in a greater cross-sectional area. This has the same effect as increasing the coil diameter in generating less heat per unit length [8].

Lastly, the dust dome attaches the top of the voice coil former to the center of the cone. Its primary function is to keep debris from entering the magnetic air gap but also serves to stiffen the moving system [1].

4.3 Electrical/Mechanical/Acoustical relationship

There are 10 key parameters for a loudspeaker. Four are mechanical, four are electrical and two are acoustical [2]. The four mechanical parameters are as follows:

1) **M**, the effective moving mass (in kilograms). Includes the mass of the cone, voice coil, voice coil former, along with small contributions from other areas.
2) **K**, the stiffness constant of the suspension (in Newtons/meter) which is dependant on the two suspension components of the driver, the surround and the spider.
3) **S**, the effective radiating area of the cone (in meters squared). This can be calculated directly from the radius of the cone and the surround (in meters). The inclusion of the surround in the calculation is because the cone has a larger surface area than a circle of the same radius and is also because, under normal operating conditions, the surround moves along with the cone [2]. A common approximation used is to take the driver size (in inches) as the effective radiator radius (in centimeters). This is usually accurate to within five percent of the actual radius [2].
4) $\mathbf{R_m}$, the mechanical resistance due to the surround and the spider (in kilograms/second).

The four key electrical parameters are:

1) $\mathbf{R_e}$, the DC resistance of the voice coil (in ohms).
2) $\mathbf{L_e}$, the self inductance of the voice coil (in Henrys).
3) **B**, the magnetic induction in the air gap where the voice coil is located (in Tesla).
4) **l,** the length of conductor in the magnetic air gap (in meters). Depending on the driver's design, the entire voice coil may or may not be inside the magnetic gap. Sometimes the coil will be deep enough to overhang the magnetic gap, keeping the length of conductor in the gap constant. Other times the coil will have a variable length of conductor in the gap due to the movement of the coil in and out of the gap [2].

The two acoustical parameters make up the overall radiation impedance. They are split into real and imaginary components since each has a different effect on the performance of the driver [2].

1) $\mathbf{R_r}$, the radiation resistance (in ohms). This is frequency dependent and also depends on the radiating surface area (**S**). This tends to be directly proportional to frequency.
2) $\mathbf{X_r}$, the imaginary component of the radiation impedance. This also depends on the radiating surface area and can increase the cone's inertia when operating at low frequencies [2].

4.4 Evaluating performance

A loudspeaker needs to be evaluated in a number of areas to give the best idea of its overall performance. The two most common methods of evaluation are the frequency response and the impedance vs. frequency relationship (**Figure 4.4**). Other important performance parameters include efficiency, sensitivity and directivity.

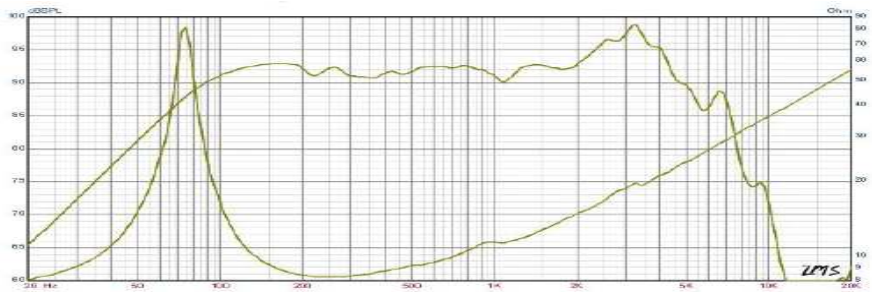

Figure 4.4: Sample frequency response & impedance chart [14]

Frequency response is easily determined by driving a loudspeaker with a logarithmic sinusoidal sweep (usually from 20 Hz to 20 kHz) with an input power of one Watt at a measurement distance of one meter [2]. The amplitude of the response is measured on a logarithmic scale in decibels (dB). An ideal loudspeaker would exhibit a perfectly flat response over the entire measured frequency range (equal measured amplitude at all frequencies). Due to the design parameters of the driver and its enclosure, though, there exist many limiting factors in performance that become apparent at different frequencies. These factors are best described using Thiele-Small parameters. These parameters, all introduced in Chapter 4.3, include:

- **a** = radiator radius
- **S** = radiator area
- **M** = moving mass
- **K** = suspension stiffness
- $\mathbf{R_m}$ = suspension resistance
- $\mathbf{R_e}$ = voice coil resistance
- $\mathbf{L_e}$ = voice coil inductance
- **B** = magnetic inductance in the air gap
- **l** = length of conductor in the air gap [2]

These parameters usually are published by driver manufacturers for use in designing loudspeaker enclosures and proper amplification and crossover systems. There are a number of equations to relate these parameters to one another. All equations are taken from Chapter 12 of [2].

First, a useful equation in enclosure design will find the ideal enclosed volume with the driver's Thiele-Small parameters. This ideal volume will theoretically give the driver the maximum linear frequency response.

$$V_o = \gamma P_o S^2 / [K(\sqrt{2}/Q_{fa})^2 - 1] \tag{4.1}$$

Where,

V_o = ideal air volume in the enclosure (m^3)

γ = 1.4, adiabatic constant for air

P_o = 1.013 x10^5 Pa, static air pressure

Q_{fa} = quality factor for free air resonance

To calculate the ideal enclosed volume, the quality factor for free air resonance must be found. This is the quality factor of the driver when it is not mounted inside the enclosure.

$$Q_{fa} = \sqrt{KM'}/[R_m + (B^2l^2)/R_e] \tag{4.2}$$

$$M' = M + \rho_o 8Sa/3\pi \tag{4.3}$$

Where,

M' = overall mass of the moving system (Kg)

ρ_o = 1.2 density of air (Kg/m^3)

Now that the ideal enclosed volume has been calculated, the rest of the theoretical performance characteristics can be calculated. It is possible to use a non-ideal enclosed volume by simply replacing the result of (4.1) with the true enclosure volume.

An important characteristic of loudspeaker performance is the resonant frequency. This is where the piston (cone) velocity is perfectly in phase with the driving voltage. This is the point where the driver is moving the fastest [2].

$$f_o = (1/2\pi)\sqrt{K'/M'} \tag{4.4}$$

$$K' = K + K_b \tag{4.5}$$

$$K_b = \gamma P_o S^2/V_o \tag{4.6}$$

Where,

f_o = resonant frequency (Hz)

K' = overall stiffness (N/m)

K_b = added enclosure stiffness (N/m)

Next, the frequency dependant acoustical pressure magnitude can be calculated by taking the magnitude of both parts of the pressure equation and multiplying the two.

$$p \approx [(V_m Bl\rho_o S)/(2\pi r M' R_e)][(-w^2/w_o^2)/(1 + jw/(Q_t w_o) - w^2/w_o^2)]e^{j(wt-kr)} \tag{4.7}$$

$$p_{mag_{part1}} = V_m Bl\rho_o S/(2\pi r M' R_e) \tag{4.8}$$

$$p_{mag_{part2}} = (w^2/w_o^2)/\sqrt{(1 - w^2/w_o^2) + w^2/(Q_t^2 w_o^2)} \tag{4.9}$$

$$p_{mag} = p_{mag_{part1}} + p_{mag_{part2}} \tag{4.10}$$

Where,

p = on-axis acoustical pressure (Pa)

V_m = driving voltage (V)

w = test frequency (rad/s)

w_o = resonant frequency (rad/s)

Q_t = total quality factor

k = wave number

r = measurement distance (m)

To find the pressure magnitude, the total quality factor must be found.

$$Q_t = w_o M'/(R_m + (B^2 l^2)/R_e) \tag{4.11}$$

Generally, a linear pressure scale is hard to analyze for loudspeaker performance. A logarithmic scale is commonly used with the pressure expressed as the sound pressure level (SPL). These values are measured in decibels (dB). There is a simple process to calculate the SPL.

$$L_p = 20log(p_{mag}/2x10^{-5}) \tag{4.12}$$

Where,

L_p = sound pressure level (dB)

In addition to SPL the axial intensity is useful for further acoustical calculations.

$$I = p^2/(\rho_o c) \tag{4.13}$$

Where,

I = axial intensity (dB)

c = 344, speed of sound in air at room temperature (m/s)

Axial intensity means that it is the radiated acoustical intensity within the ideal coverage area of a loudspeaker [2]. For example, an omni-directional loudspeaker would be on-axis anywhere around the loudspeaker, whereas a cardioid loudspeaker would have an on-axis coverage area of less than 180 degrees. With the axial intensity value known, other important loudspeaker performance parameters can be calculated.

$$P_r = I(2\pi r^2) \tag{4.14}$$

$$P_e = P_r/\eta \tag{4.15}$$

Where,

P_r = average power radiated (W)

P_e = required input electrical power (W)

To find the required input power from the power amplifier, the loudspeaker efficiency coefficient needs to be found. The efficiency coefficient is extremely important in determining the amount of heat that will be created within the voice coil. The efficiency coefficient is the ratio of input electrical power to output acoustical power [1]. If the coefficient is 0.03 (3% efficient), for example, then only 3% of the input power will become acoustical output and the remaining 97% of the input power will be converted into heat in the voice coil.

$$\eta = R_r/[(|Z_m|^2/(Bl)^2)R_e + R_m + R_r] \tag{4.16}$$

$$Z_m = R_m + (\rho_o S^2 w^2)/(2\pi c) + j[w(M + \rho_o 8Sa/3\pi - K'/w] \tag{4.17}$$

$$R_r = \rho_o S^2 w^2/(2\pi c) \tag{4.18}$$

Where,

η = efficiency coefficient

R_r = radiation resistance (Kg/s)

Z_m = mechanical impedance (Kg/s)

The mechanical impedance is generally a complex number except for the case when the test frequency equals the resonant frequency [2]. For this case it is a purely real number and will have a minimum amplitude at this point making the loudspeaker most efficient when operating at the resonant frequency. Additionally, the electrical impedance, which is also dependant on the mechanical resistance, is at its maximum at this point.

$$Z_e = R_e + jwL_e + \frac{B^2 l^2}{Z_m} \tag{4.19}$$

Where,

Z_e = electrical impedance (Ω)

The impedance spike as seen in **Figure 4.4** will result in a decrease in current within the voice coil, so there will be no increase (and possibly a slight decrease) in output at the resonant frequency. This is important to note, because in loudspeaker design it is important to maintain a flat frequency response over the desired operational frequency range.

Sometimes it is useful to create a simplified analogous circuit model of the system when only a small number of parameters are known **(Figure 4.5**). This can be used to determine the electrical impedance of the loudspeaker.

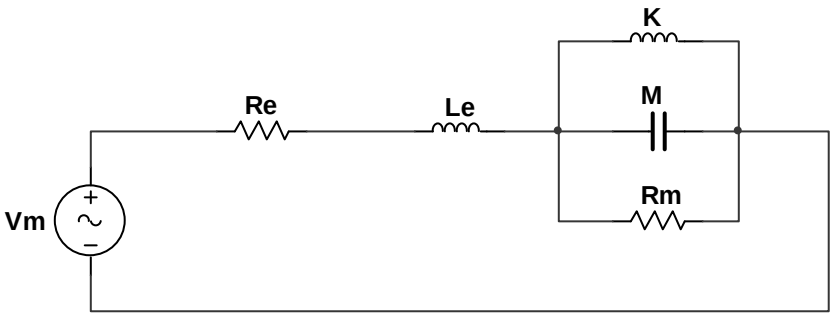

Figure 4.5: Analogous circuit model for simplified electrical impedance calculation [6]

Where,

V_m = input voltage on voice coil

$R_e(T)$ = DC voice coil resistance

α = temperature resistance coefficient

L_e = voice coil inductance

K = suspension compliance

M = moving mass

R_m = suspension resistance

After performing simple circuit analysis, the simplified electrical impedance equation is found.

$$|Z_e| = \sqrt{R_e(T)^2 + (Le + M)^2} + 1/\sqrt{R_m^2 + K^2} \tag{4.20}$$

Where,

$|Z_e|$ = magnitude of the total electrical impedance

Graphical representations of these relationships will be given in Chapter 5 (Loudspeaker Simulation).

4.5 Effects of increased voice coil temperature

An increase in voice coil temperature can have a number of adverse effects on the overall performance of a loudspeaker. The voice coil temperature directly affects the coil's resistance which in turn, affects the performance [8].

$$R_T = R_t[1 + \alpha(T_T - T_t)] \tag{4.21}$$

Where,

R_T = voice coil resistance at temperature T (Ω)

R_t = voice coil resistance at room temperature (Ω)

α = 4.33×10^{-3} temperature resistance coefficient for copper

T_T = voice coil temperature (°C)

T_t = voice coil temperature at room temperature (°C) [8]

It can be seen in (4.21) that as the voice coil temperature increases, the voice coil resistance increases. Assuming that there is a constant voltage applied to the loudspeaker, then as the voice coil resistance increases the current driven through the voice coil decreases (Ohm's Law).

$$i = V/R \tag{4.22}$$

Where,

i = current in voice coil (A)

V = driving voltage (V)

R = voice coil resistance (Ω)

The current will directly affect the mechanical force exerted on the moving mechanism of the loudspeaker (voice coil and cone) through the basic principles of magnetism where the electrical signal is converted to a mechanical signal [1].

$$f_d = Bli \tag{4.23}$$

Where,

f_d = driving piston (cone) force (N)

The force on the moving mechanism will decrease with the current. Clearly, as the voice coil temperature rises, the voice coil resistance will rise and the current moving through the voice coil will decrease, thus decreasing the overall acoustical output of the loudspeaker.

The increase in voice coil resistance will affect a number of other performance parameters along with the radiated output pressure/power including:

- V_o - the ideal enclosure volume
- K_b - the enclosure stiffness
- Q_t - the total quality factor
- Z_e - the electrical impedance
- η - the efficiency coefficient
- P_e - the input power required

The voice coil temperature affects the majority of loudspeaker performance parameters. As temperature increases the loudspeaker will output less power less efficiently and will require greater input power to maintain the necessary output level. Fortunately, loudspeakers are designed with heat dissipation in mind.

4.6 Solutions to limit voice coil temperature increase

It is known that the voice coil will rise in temperature very quickly over a short period of time but then will only have a gradual increase in temperature as it continues to operate (**Figure 4.6**) [5].

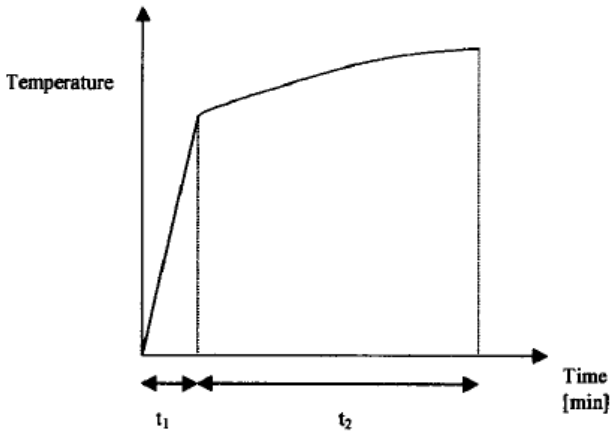

Figure 4.6: Voice coil temperature increase over time [5]

The voice coil can only dissipate heat to a certain extent on its own. The extent to which the coil can do this is characterized by its thermal resistance coefficient as seen in (4.21). This usually is not enough to keep the coil at a reasonable temperature. There needs to be additionally paths for heat to travel out and away from the voice coil. The four basic heat transfer mechanisms are as follows [9]:

1. **Conduction:** Depends on the physical heat path and the properties of the loudspeaker materials. Mostly takes place between the air enclosed in the magnetic gap and also the pole pieces.
2. **Radiation:** Depends on the surface emission rate and the surface area of the voice coil.
3. **Forced convection:** Air is vented through the voice coil as the diaphragm moves, cooling the coil.
4. **Thermal storage:** The heat is stored in surrounding materials such as the magnet structure, the back plate, and the frame. This is not necessarily considered heat transfer since it is the storage of heat, but will require these materials to release the heat at some point [9].

Without these heat transfer mechanisms, the voice coil temperature could potentially increase uncontrollably until the driver fails. This has been seen personally on a number of occasions when a loudspeaker has been heavily driven for an extended period of time. Most often, the voice coil will warp due to the great heat and will press itself against the magnet structure, thus freezing the moving mechanism in place. The only solution to this problem is to replace the voice coil structure.

Under more extreme conditions, the voice coil heat can actually cause other components of the driver to combust (generally the cone which is usually made of a paper product) (**Images 4.1 & 4.2**).

Images 4.1 & 4.2: Driver after voice coil temperature induced combustion

Generally, the pole pieces provide the best path of heat transfer from the voice coil. This is due to their close proximity to the coil inside the magnetic air gap. A common practice is to

blacken these pole pieces to maximize the heat that is routed through them from the voice coil [8].

The distance between the voice coil and the pole pieces in the magnetic gap ideally should be kept to a minimum to allow for maximum heat transfer out of the coil [8]. This must be done carefully, though, keeping voice coil thermal expansion in mind. With too small a gap between the two components, the coil could expand and begin to rub against the pole pieces resulting in the above mentioned damages.

The diameter of the voice coil must also be considered in driver design since the larger the diameter, the cooler the voice coil can stay since the generated heat is less concentrated into a single small area [8]. Additionally, the larger the air gap (both wide and deep) the greater the heat transfer capacity. The downside to this option, though, is an increase in production costs [8]. Therefore, there must be reasonable compromises between the driver performance, the heat transfer capabilities and the production costs.

Since the difference between the electrical input power and the acoustical output power equals the heat power in the voice coil, the heat transfer performance can be theoretically determined with the knowledge of key characteristics of the driver components. First, the heat power can be determined by a simple equation as long as the voice coil's DC resistance and the input current are known [9].

$$P = i^2 R_e \tag{4.24}$$

Where,

P = heat power in the voice coil

i = input current to the voice coil

R_e = DC voice coil resistance (temperature dependant)

The DC voice coil resistance will increase by approximately 0.0393% per degree Celsius (for a copper coil) [9]. To determine the transfer of this heat power out of the voice coil, a simple electrical analogous circuit can be drawn (**Figure 4.7**).

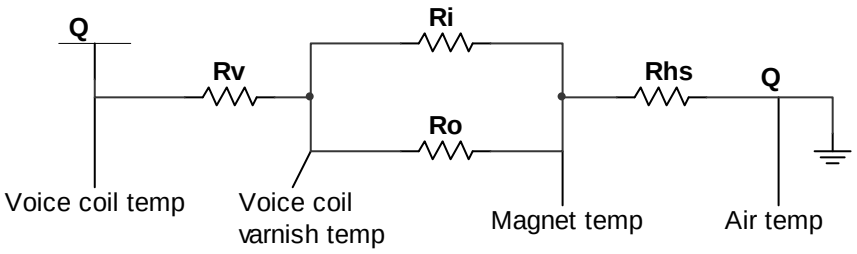

Figure 4.7: Electrical analogous circuit for heat transfer [9]

Where,

Q = heat power passing through the coil

R_v = thermal resistance of voice coil varnish

R_I = thermal resistance of heat flow in the air gap

R_o = thermal resistance from voice coil to back plate

R_{HS} = total thermal resistance of magnetic and heat sink structure

To determine the total thermal resistance of the entire system, simple circuit analysis can be performed.

$$R = R_v + \frac{R_I R_o}{R_I + R_o} + R_{HS} \tag{4.25}$$

Where,

R = total thermal resistance in the system

This now can be used to determine the amount the voice coil temperature will drop due to heat transfer and also the amount of heat energy that will be stored in each element due to the heat transfer out of the voice coil [9].

$$\Delta T = QR \tag{4.26}$$

$$E = MC\Delta T \tag{4.27}$$

Where,

ΔT = temperature drop across the element (°C)

E = heat energy stored in the heat sink structure

M = mass of the heat sink structure

C = specific heat of the heat sink structure

These relationships are key to the design of an effective driver. Without careful consideration to the heat transfer capabilities of the driver, the voice coil can have serious performance issues over time including permanent damage.

5. Loudspeaker Simulation

The purpose of the loudspeaker simulation software is to be able to theoretically predict how the loudspeaker will behave due to varying parameters. This helps to explain observations in the experimental data and possibly to explain any odd behavior at high voice coil temperatures.

5.1 Loudspeaker parameters

The Thiele-Small parameters were available for the Fane Sovereign 8-125 driver which was used for all experiments. The parameters all play a key role in the performance of the loudspeaker as discussed in Chapter 4.4. The Thiele-Small parameters are as follows [14]:

a	=	0.825 m	(radiator radius)
S	=	0.0214 m^2	(radiator area)
M	=	0.0177 kg	(moving mass)
K	=	3846 N/m	(suspension stiffness)
R_e	=	6.8 Ω	(DC voice coil resistance)
L_e	=	0.62 mH	(DC voice coil inductance)
B	=	1.0 T	(magnetic inductance)
l	=	8.6 m	(length of conductor)
f_o	=	73.9 Hz	(resonant frequency)
Q_t	=	0.70	(total quality factor)

These parameters would be used for the input to the loudspeaker simulation software and to also judge the accuracy of the simulation.

5.2 Key equations

Key equations used for the simulation software are as follows. For a complete description of these equations please refer to Chapters 4.4 and 4.5.

$$V_o = \gamma P_o S^2 / [K(\sqrt{2}/Q_{fa})^2 - 1]$$

$$Q_{fa} = \sqrt{KM'}/[R_m + (B^2 l^2)/R_e]$$

$$f_o = (1/2\pi)\sqrt{K'/M'}$$

$$p_{mag_{part1}} = V_m B l \rho_o S/(2\pi r M' R_e)$$

$$p_{mag_{part2}} = (w^2/w_o^2)/\sqrt{(1 - w^2/w_o^2) + w^2/(Q_t^2 w_o^2)}$$

$$p_{mag} = p_{mag_{part1}} + p_{mag_{part2}}$$

$$Q_t = w_o M'/(R_m + (B^2 l^2)/R_e)$$

$$L_p = 20log(p_{mag}/2x10^{-5})$$

$$I = p^2/(\rho_o c)$$

$$P_r = I(2\pi r^2)$$

$$P_e = P_r/\eta$$

$$\eta = R_r/[(|Z_m|^2/(Bl)^2)R_e + R_m + R_r]$$

$$Z_m = R_m + (\rho_o S^2 w^2)/(2\pi c) + j[w(M + \rho_o 8Sa/3\pi - K'/w]$$

$$Z_e = R_e + jwl + B^2 l^2/Z_m$$

$$R_T = R_t[1 + \alpha(T_T - T_t)]$$

Where,

V_o	=	ideal enclosed air volume (m^3)
Q_{fa}	=	free air quality factor
f_o	=	resonant frequency
p_{mag}	=	pressure magnitude (Pa)
Q_t	=	total quality factor
L_p	=	axial sound pressure level (dB)
I	=	axial intensity (dB)
P_r	=	average power radiated (W)
P_e	=	required input power (W)
η	=	efficiency ratio
Z_m	=	mechanical impedance (Kg/s)
Z_e	=	electrical impedance (Ω)
R_T	=	DC voice coil resistance due to temperature (Ω)

5.3 Overview of MATLAB software

The MATLAB simulation software was created to allow the user with a good deal of flexibility in adjusting parameters to determine a loudspeaker's theoretical performance. The input parameters can be any real number. One of these parameters can be set to sweep over a specified range of values. This is especially helpful to determine performance over the audible frequency band of approximately 20 – 20,000 Hz. It could also be useful to sweep the voice coil temperature to examine the effects of temperature on performance.

The user is also allowed to select the method of enclosure volume calculation. The first option is to use the calculated ideal enclosed air volume. This will give the loudspeaker optimally flat response over the frequency range. Alternatively, the user can enter the dimensions of the enclosure or directly enter the volume of the enclosure.

Once all the parameters have been defined the user can select the number of measurement points to be taken during the one parameter sweep and the scale for the plotting (linear or logarithmic). Once the calculations are finished, the user has a number of plotting options to view the relationships between the swept parameter and the performance characteristics of the loudspeaker (**Figure 5.1**).

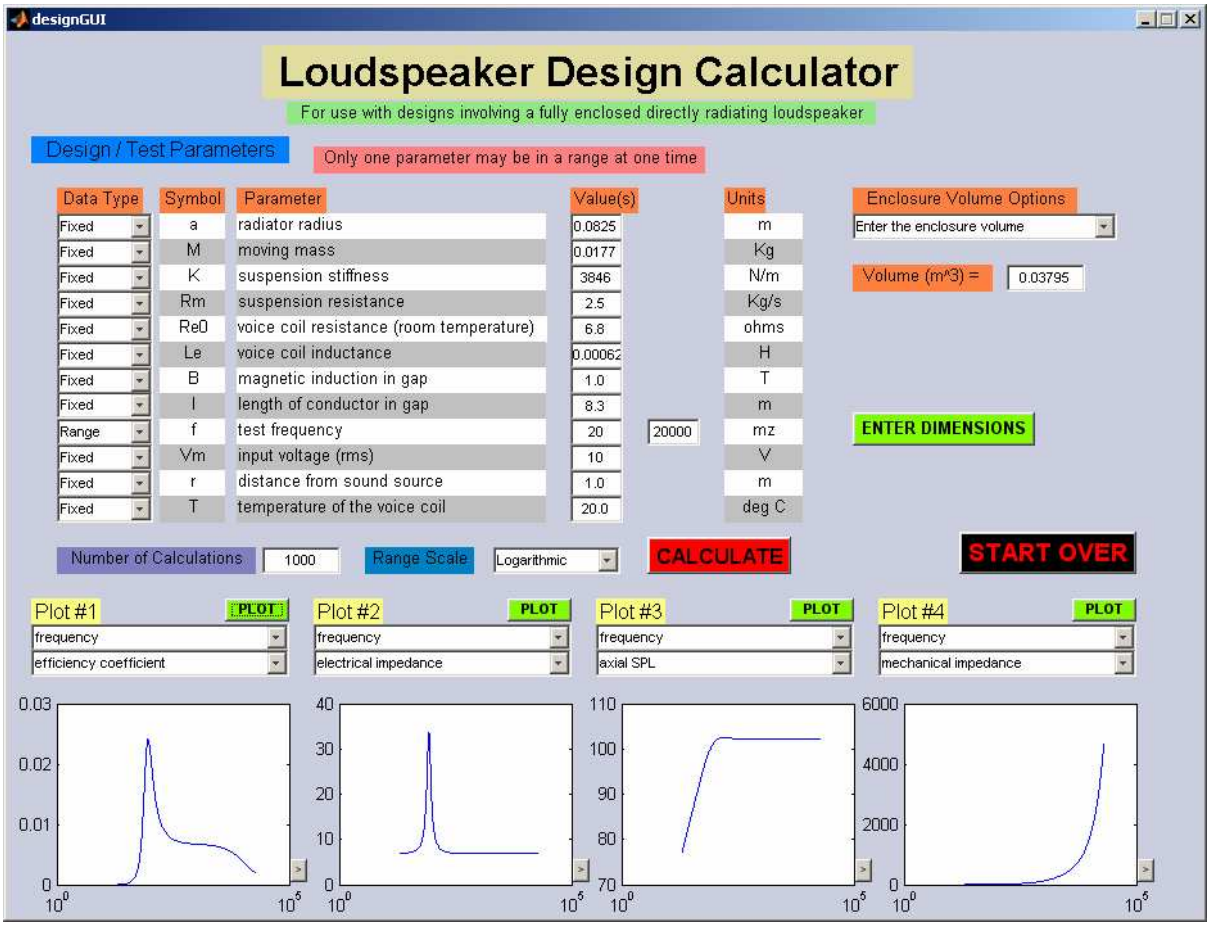

Figure 5.1: Loudspeaker simulation tool (w/ Sovereign 8-125 Thiele-Small parameters)

5.4 Simulation results

A number of simulations were performed using the Thiele-Small parameters of the Sovereign 8-125 driver that was used for the loudspeaker testing. Frequency was swept using a range from 20 – 20,000 Hz. The three values that were plotted versus frequency were efficiency coefficient, electrical impedance and axial SPL.

These values were examined with a range of voice coil temperatures from 20 °C to 100 °C. At these temperatures, the efficiency and electrical impedance are at their peak around 90 Hz (**Figures 5.2 & 5.3**). This indicates that the loudspeaker's resonant frequency is close to 90 Hz. This is close to the manufacturer's specification of a resonant frequency at 73.9 Hz. The difference is due to the effects of the enclosure [16].

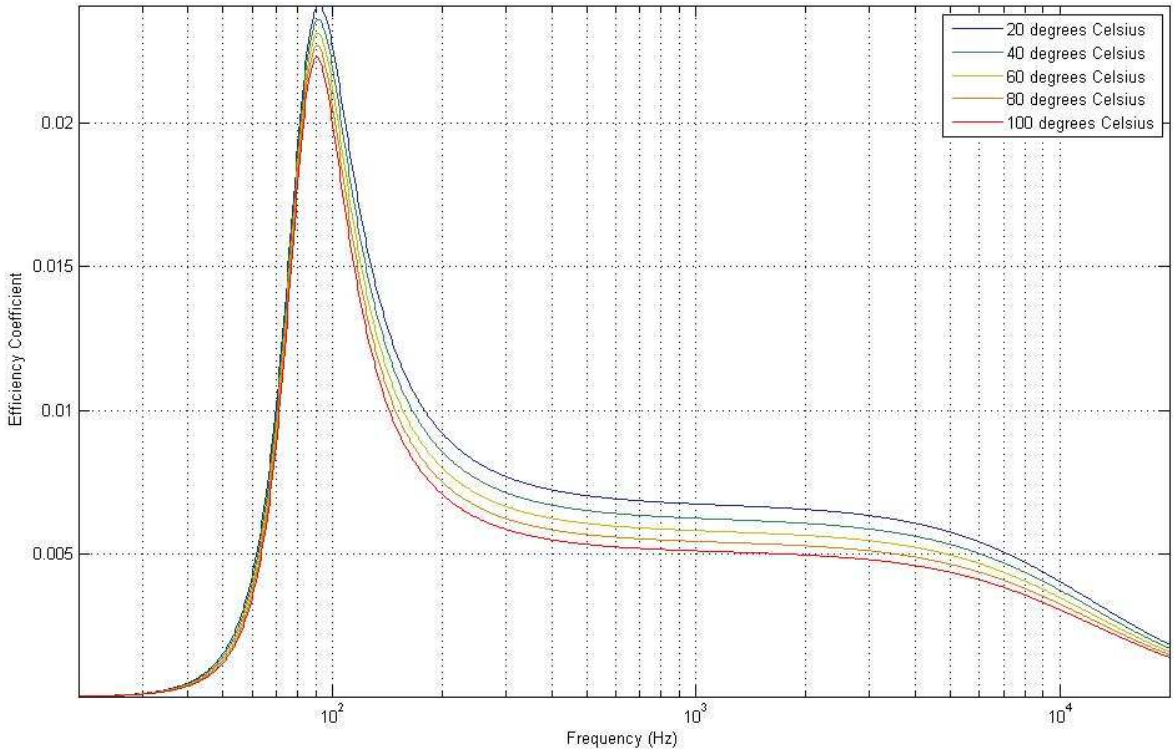

Figure 5.2: Efficiency coefficient vs. frequency calculation

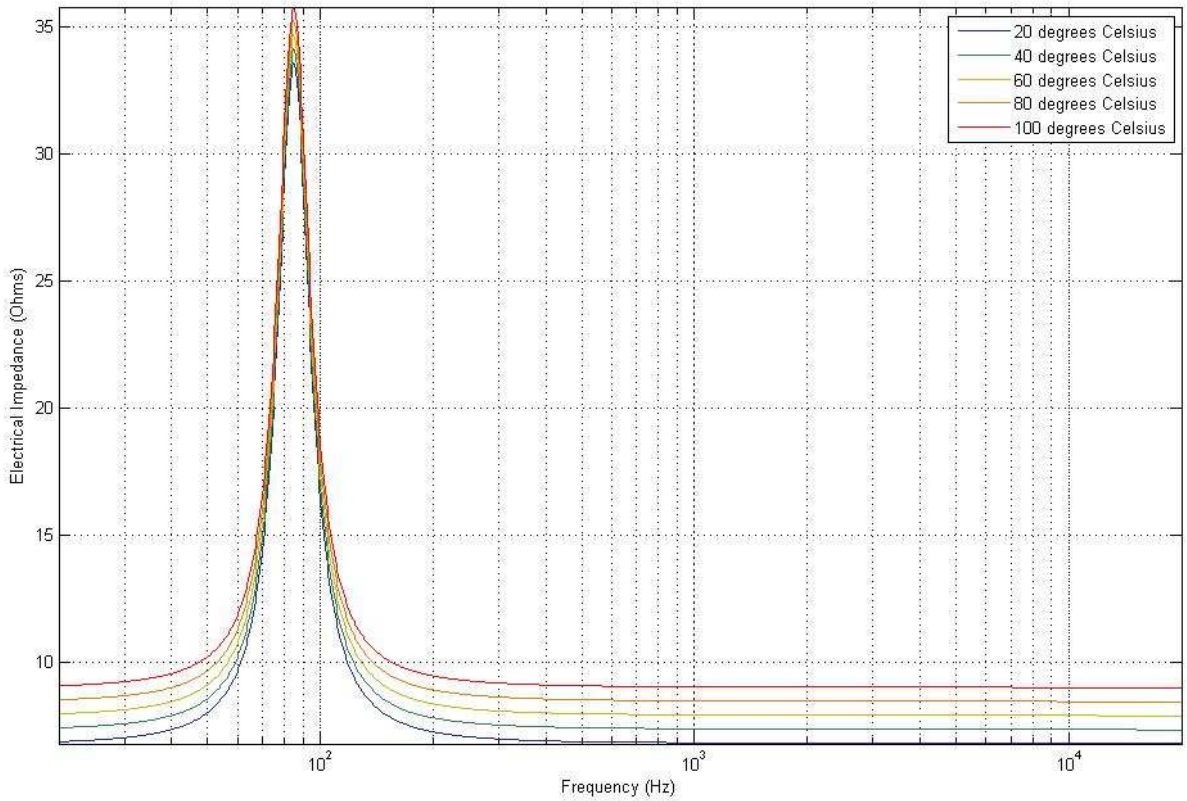

Figure 5.3: Electrical impedance vs. frequency calculation

Upon examining the axial SPL behavior as the voice coil temperature increases (**Figure 5.4**) a noticeable non-linearity appears just above 100 Hz. At 100 °C the frequency is 2 dB greater in SPL than the rest of the frequency range. If this is a valid simulation, then this heightened response around 100 Hz at high voice coil temperatures should appear in the experimental results in Chapter 6.

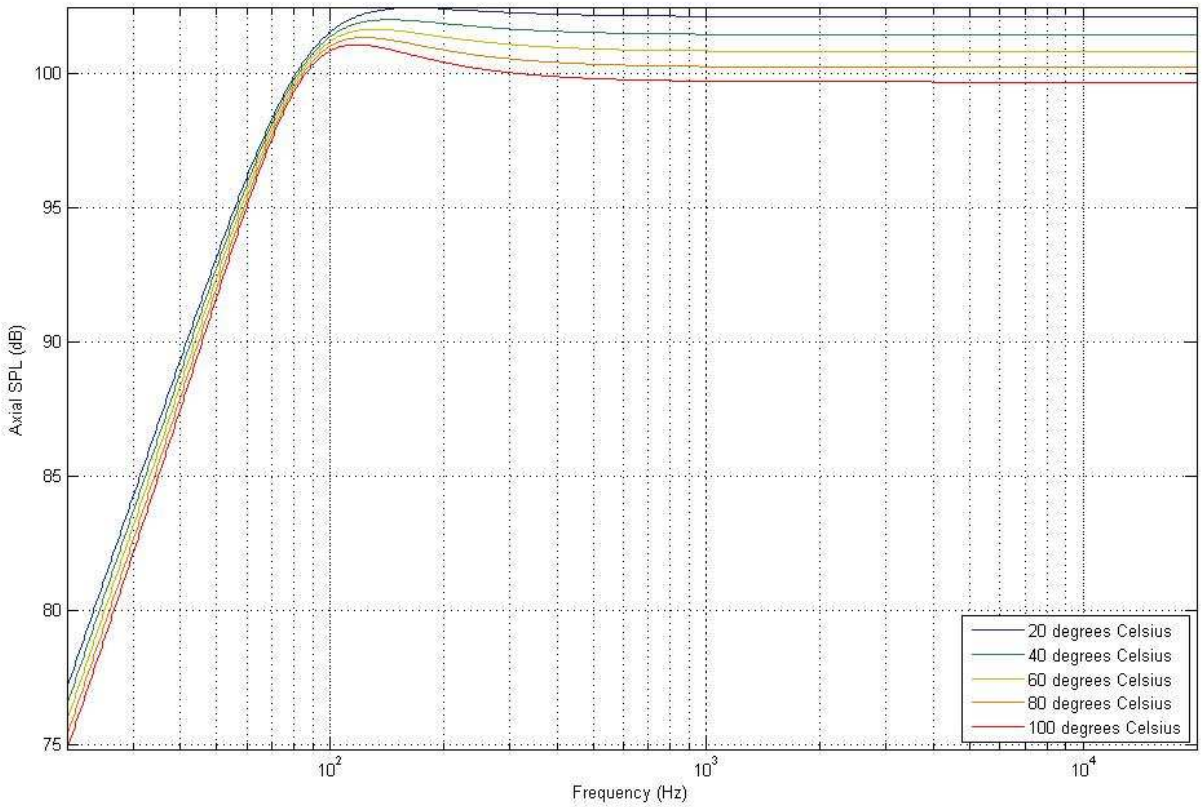

Figure 5.4: Axial SPL vs. frequency calculation

At room temperature, the efficiency peaks just over 2.5%, but now at this higher voice coil temperature the efficiency is 2.25%, meaning heat is being generated at a greater rate than at room temperature. This decrease in efficiency results in the overall decrease in axial SPL (**Figure 5.4**) of about 3 dB.

Voice coil temperature plays a key factor in the overall loudspeaker performance. As the temperature rises, the loudspeaker becomes less efficient in converting the input electrical power into acoustical power. This results in a decrease in the output SPL and a slightly worsened frequency response and more heat generated within the driver.

5.5 Limiting factors of the simulation

This simulation was created using only basic loudspeaker equations. It does not take into account a number of aspects of the loudspeaker design including the enclosure geometry, any insulation inside the enclosure, ports installed in the loudspeaker or the factory specified frequency response of the driver. A more advanced piece of simulation software would be required to get extremely accurate results. For this project, though, only approximate behavior plots are needed to help explain the experimental results.

6. Loudspeaker Experimentation

The loudspeaker measurements are the focus of this project. Over the course of the research period, a measurement technique was developed and refined using existing loudspeaker measurement techniques and then combined into one functional piece of software. The purpose of the experiments were to directly explore the effects of voice coil temperature on loudspeaker performance.

6.1 Measurement techniques

In experimentation it is important to be able to validate measurements. In this situation, it was necessary to utilize two completely different measurement techniques that would hopefully give agreeing results. Agreeing results would allow for confident analysis of data without doubt of validity.

6.1.1 Maximum length sequences

A common technique often used in acoustical measurements is the use of Maximum Length Sequences (MLS). This technique is useful for situations where the signal to noise ratio is low to the point where a direct impulse response cannot be measured. The MLS is a pseudo-random binary signal that consists of repeatable signal that at first glace may seem completely random [3]. The signal is generated using a feedback shift register whose values are determined using known recursion relations.

To better illustrate, take the example of the generation of an MLS signal of the 4th order [3]. First, the recursion relation must be stated:

$$h(x) = x^4 + x + 1 \tag{6.1}$$

This recursion relation can now be applied to the shift register to generate the MLS.

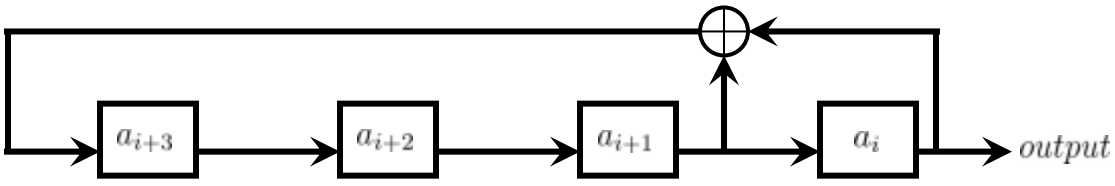

Figure 6.1: Block diagram for a 4th order MLS shift register [3]

The a_i term in the diagram relates to the 1 in (6.1). The a_{i+1} term relates to x. To find next term (a_{i+4}) a_{i+1} and a_i are put through an exclusive or (XOR) operator. This means that the

output will only equal one when either a_{i+1} or a_i equals one. If both or neither equal one, then the output will be zero. The output vector will be generated from the elements shifted out of the register on the right hand side. The initial condition used for this project will be ones for all elements. Any initial conditions can be used, though, with the exception of all zeros because in that case the XOR output would always equal zero, giving an output vector of all zeros [3].

The length of the output vector is directly determined by the order of the sequence.

$$N = 2^m - 1 \tag{6.2}$$

Where,

N = the length of the sequence

m = the order of the MLS

In this case, the length of the sequence will be 15. This means that the shift register will cycle through fifteen different states before returning to its initial state of all ones. It then repeats itself. To make the signal best suited for a loudspeaker system, the signal needs to be converted to a -1 to 1 scale to allow for full loudspeaker movement [3]. In the signal's current state, the loudspeaker would only move from its equilibrium position outward. With this new scale the loudspeaker can move within its entire range.

$$s_0, s_1, s_2, ... = (-1)^{a_0}, (-1)^{a_1}, (-1)^{a_2}, ... \tag{6.3}$$

Where,

s_i = adjusted MLS element (-1 to 1 scale)

a_i = raw MLS element (0 to 1 scale)

Now that the MLS vector has been created it can be sent through the system for measurement. It is important to note that the MLS must be played twice in order to avoid an unwanted impulse spike at the beginning of the signal due to the system being excited from rest [3]. After recording the MLS played twice, the first pass of the sequence can be discarded and the second pass can be used as the measurement.

It is a simple process to extract the impulse response of the system. The goal will be to extract the system impulse response, h, from the MLS signal, s, and the measured signal, y. It is known that the measured signal is a result of convolution of the input with the system response [3].

$$y = s * h \tag{6.4}$$

Next, correlation is performed on the entire equation with respect to the MLS signal.

$$\phi_{sy} = \phi_{ss} * h \tag{6.5}$$

The correlation of the MLS with itself (auto-correlation) equals one, meaning that the MLS is exactly the same as itself. Now all that is left is a simple equation to find the system impulse response, h [7].

$$h = \phi_{sy} \tag{6.6}$$

This means that once the measurement has been taken, all that needs to be done is to find the correlation between the input and output signals. This should give the impulse response of the system.

Using only one variation of MLS signal is not always sufficient. This is due to the presence of harmonic distortion in measurements. A simple solution to this problem is to generate five different MLS signals from five different recursion relations [15]. Once the five MLS signals are measured they can be averaged to remove any unwanted distortion. This is accomplished by averaging the measurements, discarding the maximum and minimum values for each time step. This takes the measured signal spikes out of the averaging calculation, thus removing the distortion (**Figure 6.2 & 6.3**) [15].

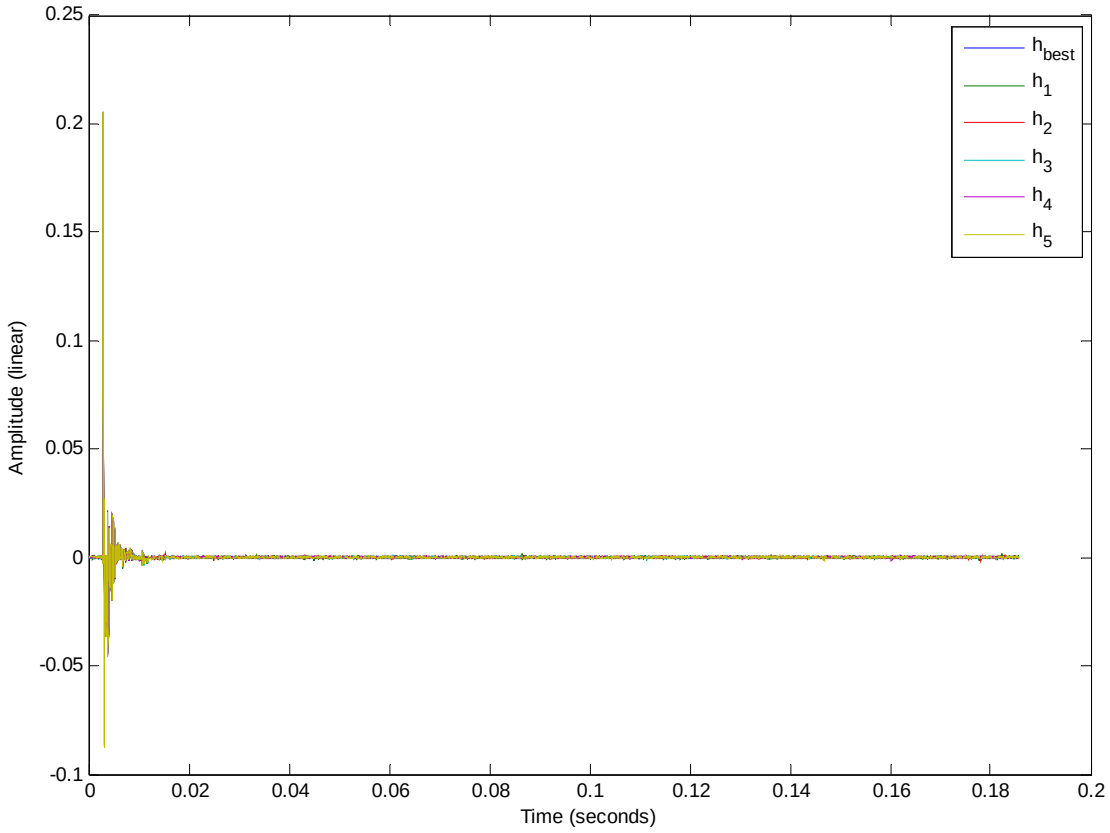

Figure 6.2: 5 MLS signals w/averaged "best" response (July 27, 2008 meas. data)

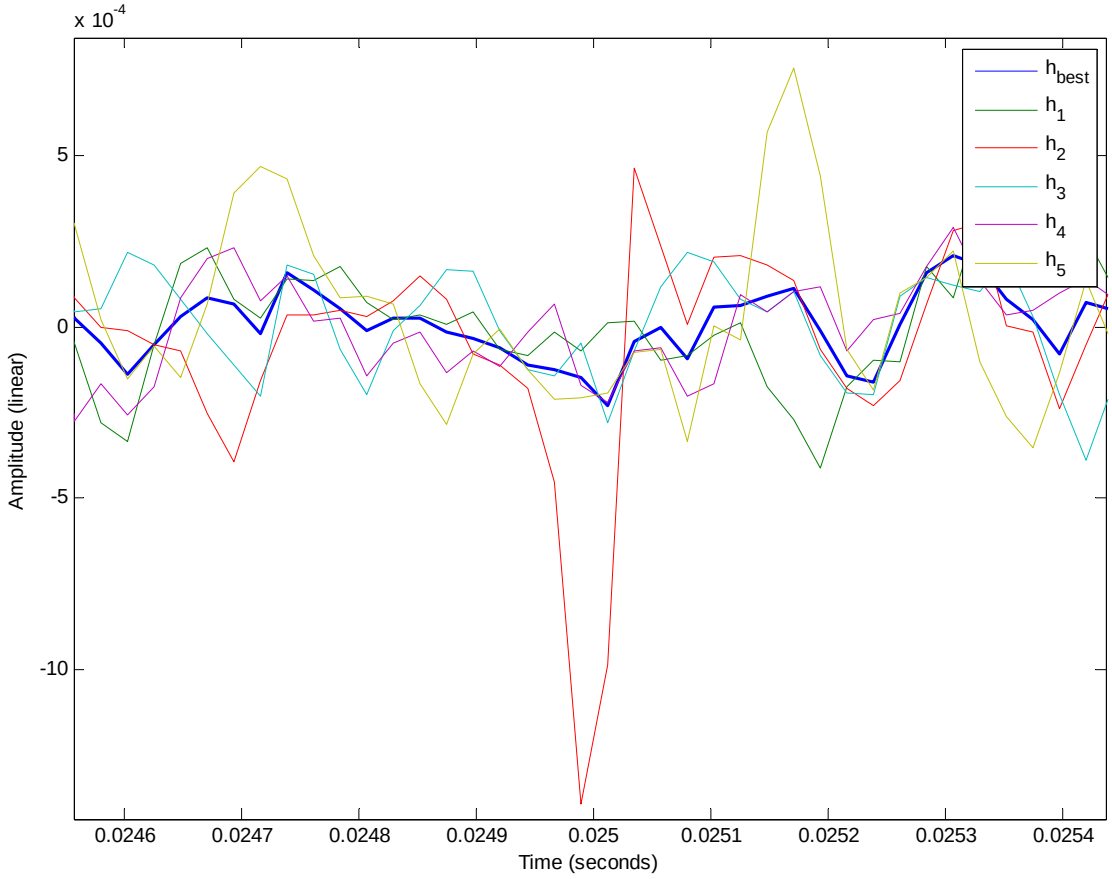

Figure 6.3: Magnification of Figure 6.2 to highlight MLS averaging

Once the impulse responses are measured and averaged to remove distortion they can be used to find the frequency response of the system. This is done with a Fast Fourier Transform function (FFT).

6.1.2 Sinus-Logarithmic sweep

The sinus logarithmic sweep is an extremely efficient technique to determine the frequency response of a system. This technique involves creating a logarithmic sweep in frequency starting and ending at given frequencies over a set period of time. There are techniques for taking this sweep measurement and extracting the system impulse response [10], but for this project the frequency response is only of interest so the further calculation is not necessary. The sweep can be generated with a single equation (6.7) [10] and once measured, can be immediately used for analysis without any further calculations.

$$x(t) = sin[\frac{(2\pi f_{min} T)}{ln(f_{min}/f_{max})}(e^{\frac{t}{T}ln(\frac{f_{min}}{f_{max}})} - 1)] \tag{6.7}$$

Where,

$x(t)$ = logarithmic sweep signal

f_{min} = starting frequency (Hz)

f_{max} = ending frequency (Hz)

T = duration of the sweep (seconds)

6.2 Software overview

The software created to take both the MLS and sweep measurements was written in MATLAB. All software is completely original using key equations from [3], [7], [10] and [15]. The software was written to allow for easy use. A user would need to connect the output from the mixer (with the measurement microphone connected) to the microphone jack on any MATLAB-equipped PC and then connect the sound output of the PC to the amplifier (or mixer first) driving the loudspeaker. The only additional configuration needed would be to set the input and output levels of the PC's sound card to avoid any clipping.

6.2.1 Maximum length sequences

Since the measurements for this project were all carried out in an anechoic chamber, the duration of the MLS signals used did not have to be very long. This is because there is no room response due to the signal so all that is being measured is the direct response of the loudspeaker. With this in mind, an MLS signal of order 13 was chosen. This MLS signal has $2^{13} - 1 = 8191$ samples. A sample rate of 44100 Hz would correspond to a signal with a duration of 0.186 seconds. Since five MLS signals were used, each being played twice, the duration of the full test signal was 1.86 seconds.

Since this experiment called for five different 13th order MLS signals, it was necessary to find five different recursion relations for the generation of the signals [15].

$$a(i+13) = a(i+4) + a(i+3) + a(i+1) + a(i) \tag{6.8}$$

$$a(i+13) = a(i+10) + a(i+9) + a(i+7) + a(i+5) + a(i+4) + a(i) \tag{6.9}$$

$$a(i+13) = a(i+11) + a(i+8) + a(i+7) + a(i+4) + a(i+1) + a(i) \tag{6.10}$$

$$a(i+13) = a(i+10) + a(i+9) + a(i+8) + a(i+6) + a(i+3) + a(i+2) + a(i+1) + a(i) \tag{6.11}$$

$$a(i+13) = a(i+12) + a(i+10) + a(i+9) + a(i) \tag{6.12}$$

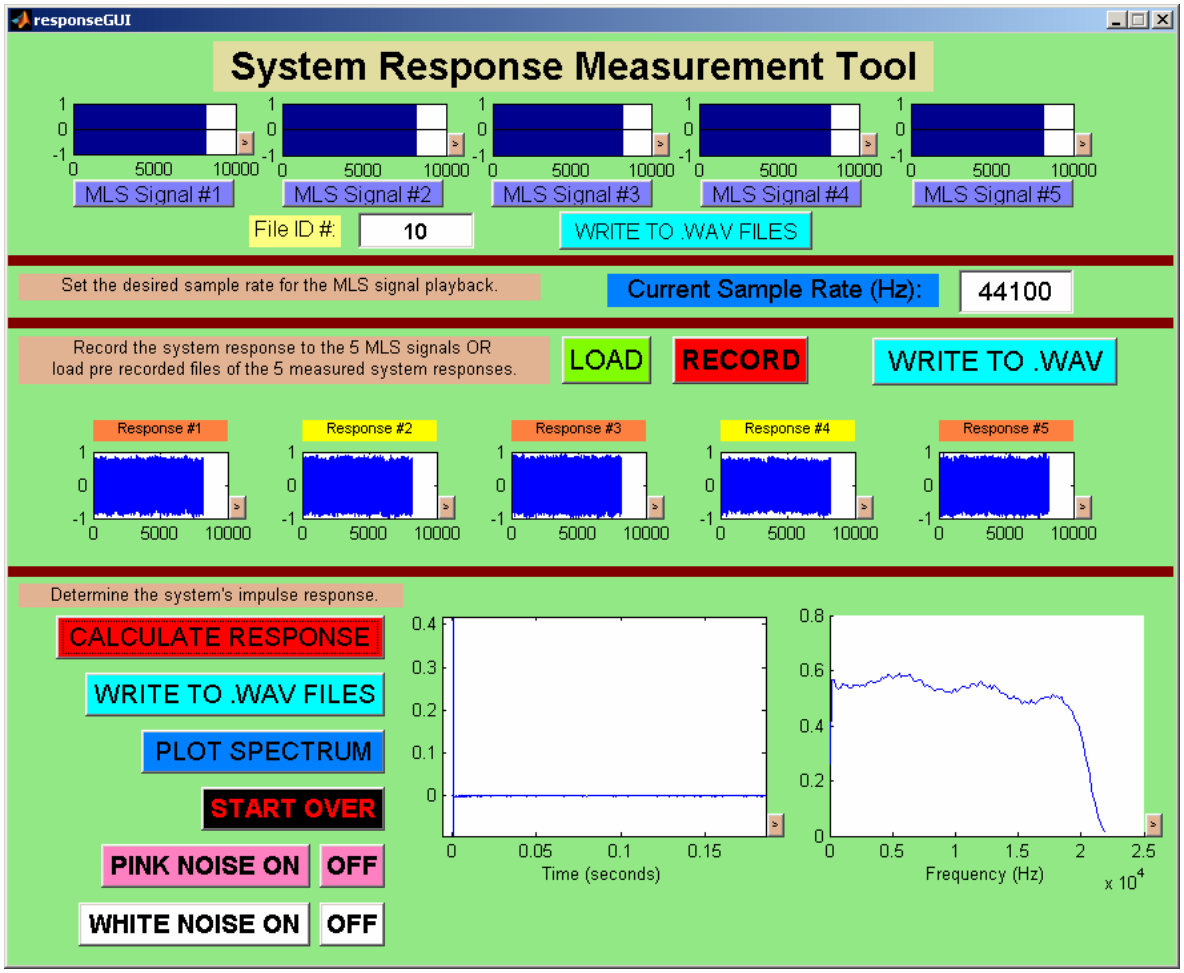

Figure 6.4: Initial MLS measurement tool GUI (measurement of PC sound card)

The initial version of the MLS measurement tool gave a user a number of options (**Figure 6.4**). The program first generates the five MLS signals. These can be played back by clicking the buttons below the MLS plots and can be written to .wav files. The user can define both the sampling rate and the identification number to be used with the current measurement which will be used when writing the data to .wav files.

Next, the MLS measurements can be made by clicking the record button or previous measurements can be loaded for further analysis by clicking the load button. Once the measurements are present, "CALCULATE RESPONSE" can be clicked to extract the impulse response of the system to calculate the frequency response.

Once this has been done, the results can be written to .wav files and also expanded magnitude and phase spectra can be plotted (**Figure 6.5**). This program also allows for the playback of

pink and white noise. This is used to drive the loudspeaker between measurements, causing the voice coil temperature to rise.

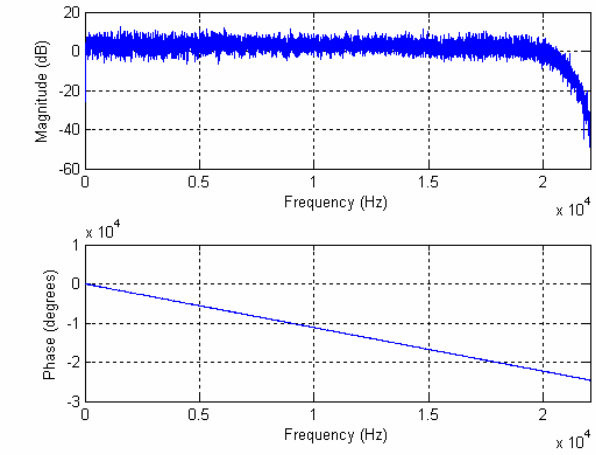

Figure 6.5: Magnitude and phase spectra of PC sound card MLS measurement

Since all measurements were set up identically, the MLS measurement tool was simplified to automatically play the MLS signals, take the measurements and analyze the data when the start button was clicked (**Figure 6.6**). Again, this GUI allowed for expanded spectra plotting and .wav file writing using the user-defined identification number.

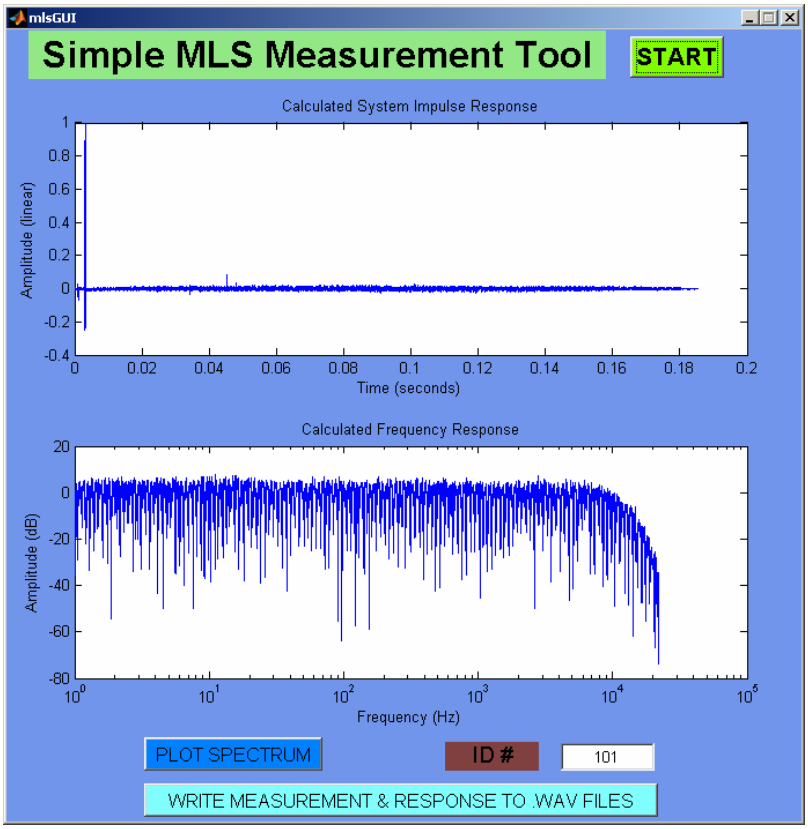

Figure 6.6: Simplified MLS measurement tool (measurement of PC sound card)

Both MLS measurement tools utilize the wavrecord function in MATLAB to record the measurements and the corr function to extract the impulse response from the measurement. A disadvantage to the simplified MLS measurement tool is that it does not offer the option to playback pink or white noise. This issue is addressed for the final software package (Chapter 6.2.3).

6.2.2 Sinus-Logarithmic sweep

The logarithmic sweep software is fairly simple to implement in MATLAB using only one equation (6.7) to generate the sound vector. In the initial implementation of the software, the sweep is recorded and then three relevant plots are created. First is the plot of the direct sweep signal in the time domain. Next the same signal is plotted, but on the decibel scale. Finally, the signal is analyzed through Fast Fourier Transform, resulting in the frequency response plot (**Figure 6.7**).

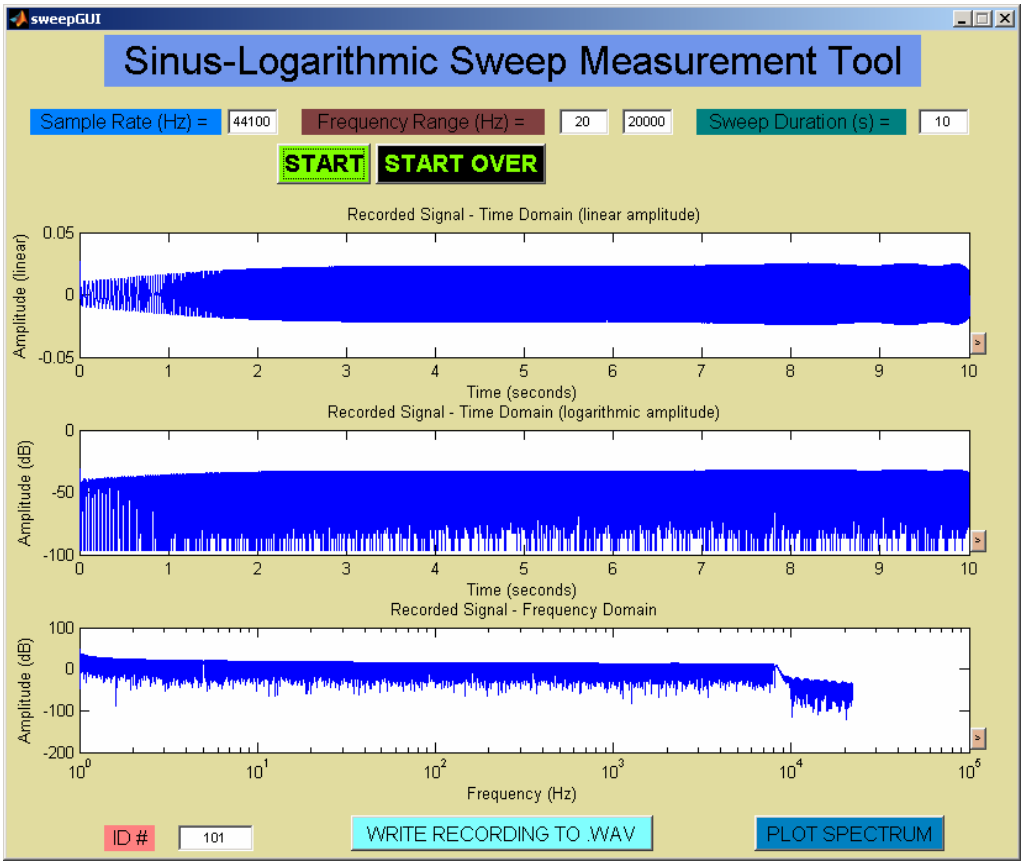

Figure 6.7: Initial logarithmic sweep tool (measurement of PC sound card)

This program also allows for the plotting of the magnitude and phase spectra using MATLAB's freqz operation (**Figure 6.8**). This tool helps to validate the third plot in Figure 6.5 and gives a clear representation of the frequency response.

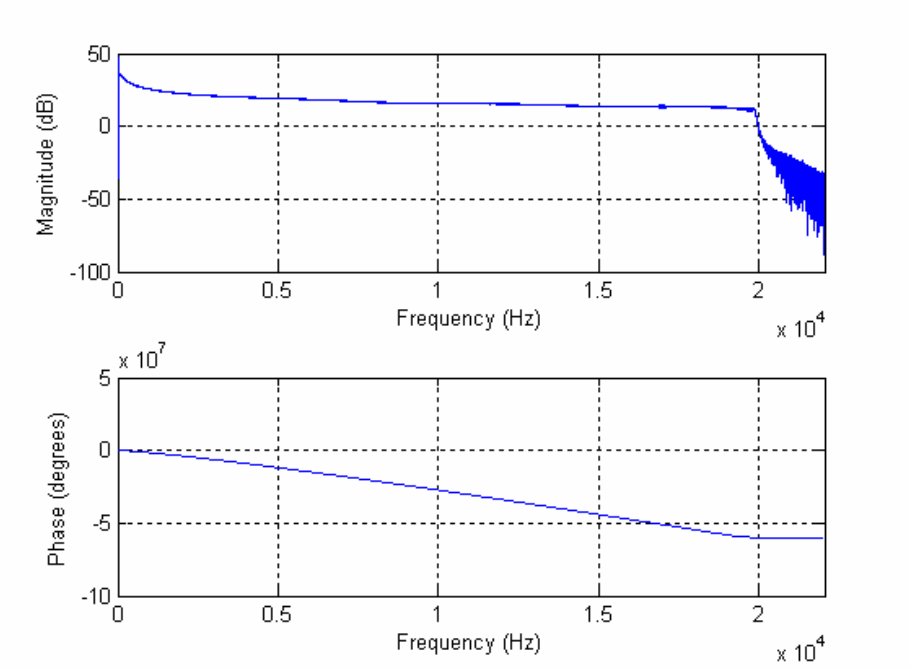

Figure 6.8: Magnitude and phase spectra for PC sound card sweep measurement

6.2.3 Final measurement software package

The final MATLAB software package created to perform the loudspeaker measurements is a combination of the MLS and logarithmic sweep software. The two types of measurements were combined to be performed one after the other. When the two measurements are finished, the user is prompted to rotate the loudspeaker to the next measurement angle (0°, 30°, 60° or 90°). The measurements are repeated for these positions until they have all been covered. Once the final measurement has been taken, the software will plot the MLS and sweep measurements in the open window. This allows for the user to verify that they were recorded and processed properly.

Once all measurements have been taken, white noise can be played for a user-determined length of time in minutes. Once the noise is finished playing a new set of measurements can be taken. This can be repeated as many times as necessary (**Figure 6.9**).

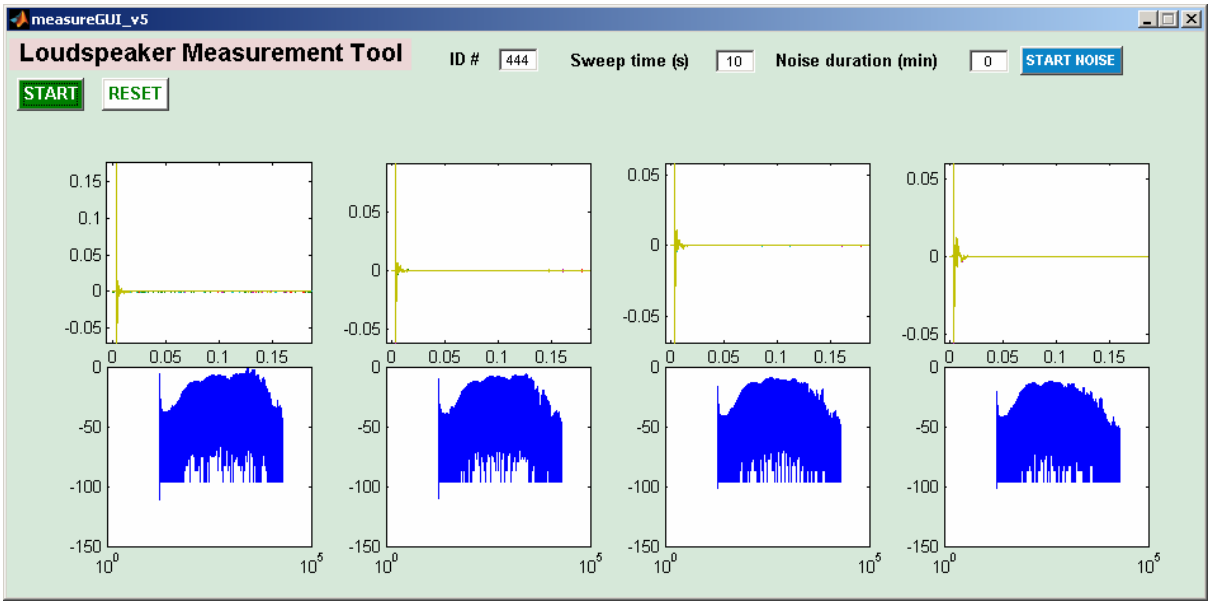

Figure 6.9: Final loudspeaker measurement tool (displaying one set of measurements)

Next, software to perform the data analysis was created (**Figure 6.10**). This software allows for direct comparison of two measurements at a time. The user first loads the data set from the loudspeaker measurement tool. Once the data has been loaded, the software will generate a plot of measured temperature, measured voice coil resistance and calculated voice coil temperature as a function of time.

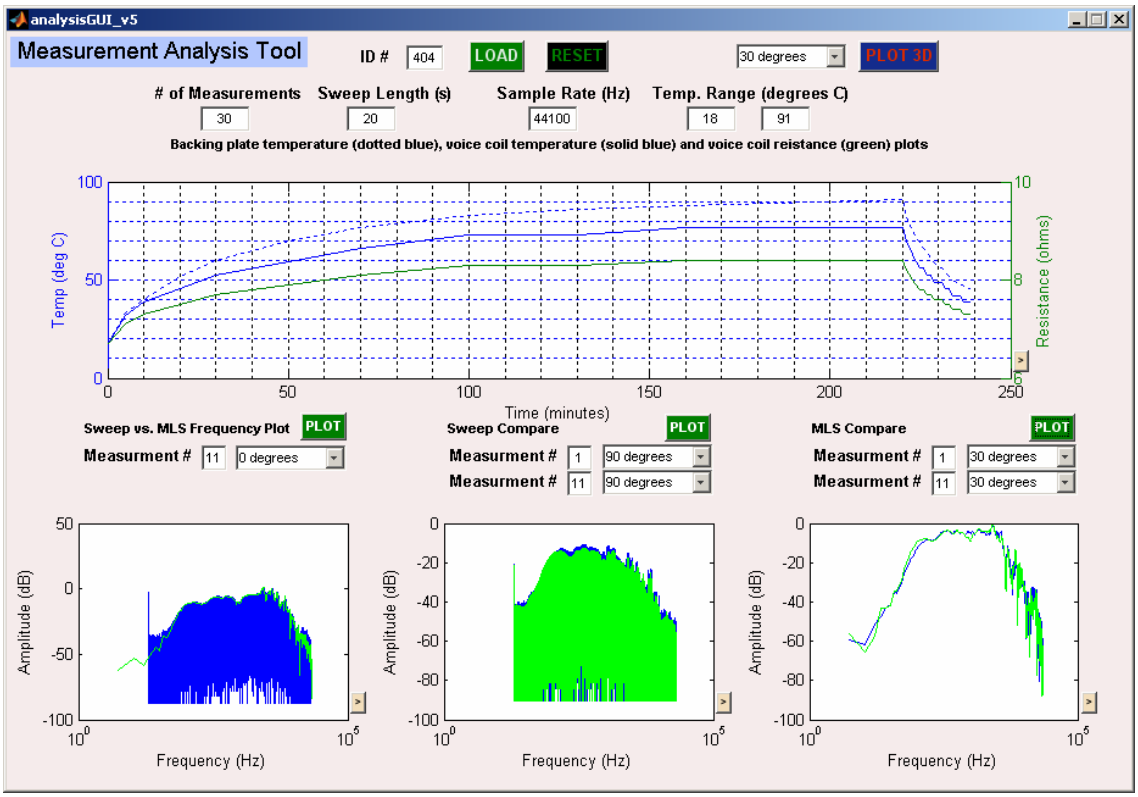

Figure 6.10: Final measurement analysis tool (displaying analysis from anechoic chamber measurements of the loudspeaker on August 1, 2008)

Now the user can choose which measurement numbers to plot and compare. The software allows for the plots to be expanded into a separate window for detailed examination. This software is extremely useful for a number of reasons:

1) MLS and sweep measurement agreement verification
2) direct comparison of MLS and sweep measurements from different data sets
3) ability to determine voice coil temperature effects on the frequency response at varying measurement positions and voice coil temperatures

6.3 Experimental setup

Experimentation was performed in an anechoic chamber to eliminate the possibility of room effects on the measurements. This would ensure that only the loudspeaker's response to the input signal was measured. It also made the experiments easily repeatable.

6.3.1 Hardware utilized

All signals were generated and transmitted through a PC's sound card that was directly connected to a Tascam M-08 mixing console (**Image 6.1**). The signal was routed to only the left channel of the console's output. This was fed into a Sherwood AX-3030R power amplifier with an 8 ohm output (**Image 6.2**) which was connected directly to the loudspeaker in the anechoic chamber. The loudspeaker used was a Tannoy 607.

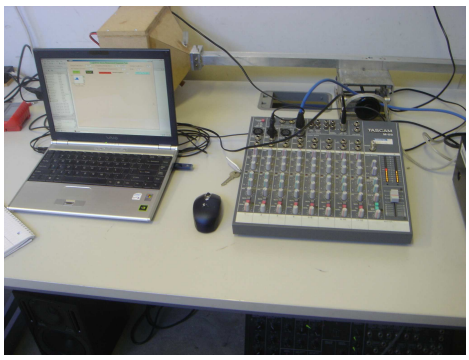

Image 6.1: Computer & mixer setup

Image 6.2: Power amp setup

The 607 had a single 8" driver for low and mid frequencies and a tweeter for the highs. To simplify the experiments, the tweeter was disconnected from the system and the passive crossover circuitry was bypassed to allow for a direct connection to the 8" driver.

The original 8” driver was rated at 8 ohms with unknown Thiele-Small parameters. This driver’s voice coil ended up warping after only a few experimental runs. It was replaced by a Fane Sovereign 8-125 8” driver (8 ohms). This driver came with Thiele-Small parameters and also had a design that made for easier temperature readings (**Images 6.3 & 6.4**). All results presented in this paper were obtained by measuring this driver only.

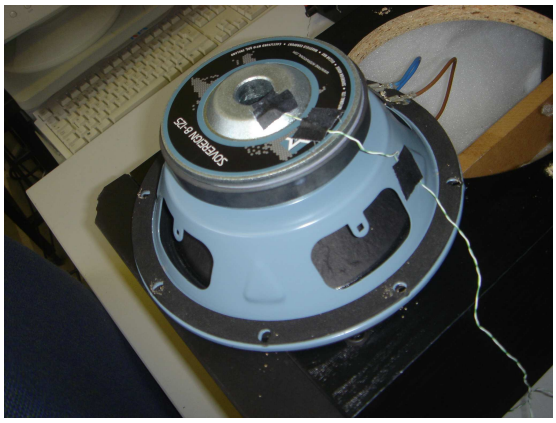

Image 6.3: Sovereign 8-125 rear

Image 6.4: Sovereign 8-125 in the enclosure

A Neumann KM-184 condenser microphone with known frequency response (**Figure 6.11**) was used for all measurements. This was placed on a mic stand exactly one meter from the driver’s dust dome and on the same horizontal plane at the exact center of the driver. The output from the microphone ran back into the Tascam mixer and was routed to the right output channel. This was directly connected to sound card’s input.

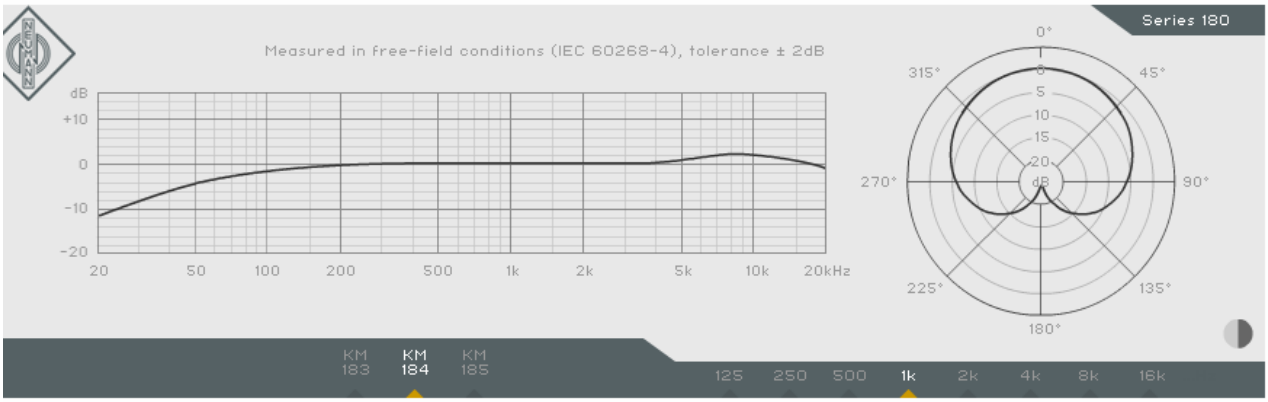

Figure 6.11: Neumann KM-184 frequency response from 20 Hz to 20 kHz and polar pattern at 1 kHz (courtesy of www.neumann.com)

6.3.2 Positioning and settings

The main output of the mixer was run at 0 dB and the amp was set to 100% power to avoid any internal attenuation effects in the amplifier circuitry. The test signal level was controlled

through the computer software and the recorded signal from the microphone was controlled by the head amp on the channel strip of the mixer.

All settings were kept identical for all measurements. The only setup variable was the orientation of the loudspeaker. Four positions were used: 0° (directly on axis), 30°, 60° and 90° (directly to the side of the loudspeaker). The microphone was kept stationary at all times while the loudspeaker was rotated to the required angle (**Image 6.5**).

Image 6.5: Microphone & loudspeaker setup

The frequency response of the sound card alone (**Figure 6.12**) and the sound card through the Tascam mixer (**Figure 6.13**) were measured using an MLS and a logarithmic sweep.

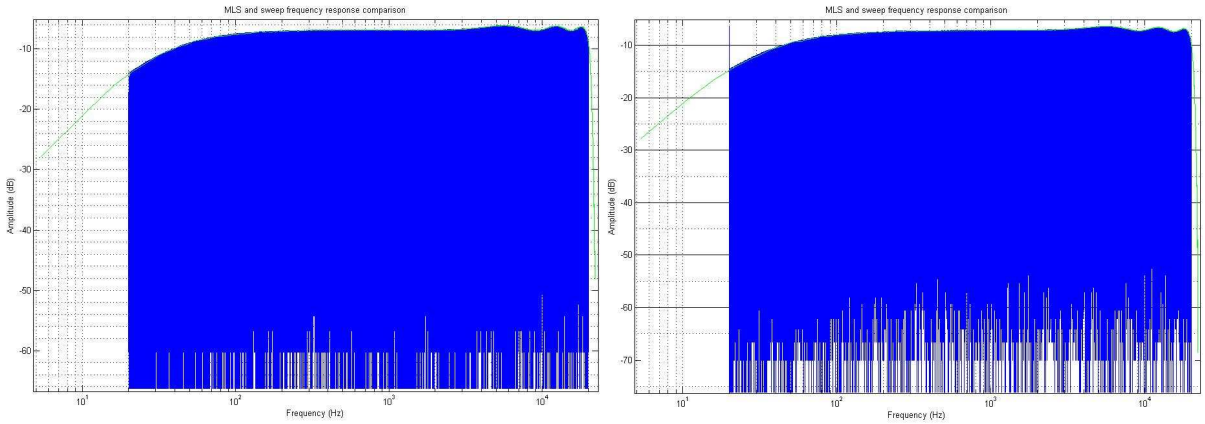

Figure 6.12 (left): Measured sound card frequency response

Figure 6.13 (right): Measured sound card + Tascam mixer frequency response (green = MLS, blue = sweep)

The above figures show that the sound card adds a gradual amplitude roll off as the frequency drops below 100 Hz. There is a roughly 15 dB drop from 100 Hz down to 10 Hz. This drop off must be taken into consideration when analyzing the loudspeaker measurements, but as long as the same mixer and sound card combination are used in all measurements, this drop off should not negatively impact the results.

6.3.3 Drawbacks and limitations

There were a number of drawbacks and limitations during the experimental process. With the available equipment, it was impossible to directly measure the voice coil temperature. Instead, a thermocouple was placed very close to the voice coil on the magnetic structure. This gave a reading that gave a good idea of the heat transfer that was taking place in the driver. To find the actual voice coil temperature, the DC voice coil resistance had to be monitored and then used to calculate the temperature.

Another time consuming situation involved what is now believed to be a problem with the sound card of the initial computer used to take the measurements. The MLS measurements never seemed to line up correctly. They seemed to have additional data from each MLS signal recording. This caused the correlation calculation to result in little to no correlation, giving no clear impulse response. This problem was resolved by using a different computer. A considerable amount of time was spent examining the software before it was determined that it was a hardware problem. Once this issue was resolved, measurements had to be completely redone.

7. Experimental results and analysis

The analysis tool created for this project (**Figure 6.10**) allows for a number of different methods of data analysis through plotting. First, the measured temperature, calculated voice coil temperature and DC voice coil resistance versus time plot was created (**Figure 6.14**).

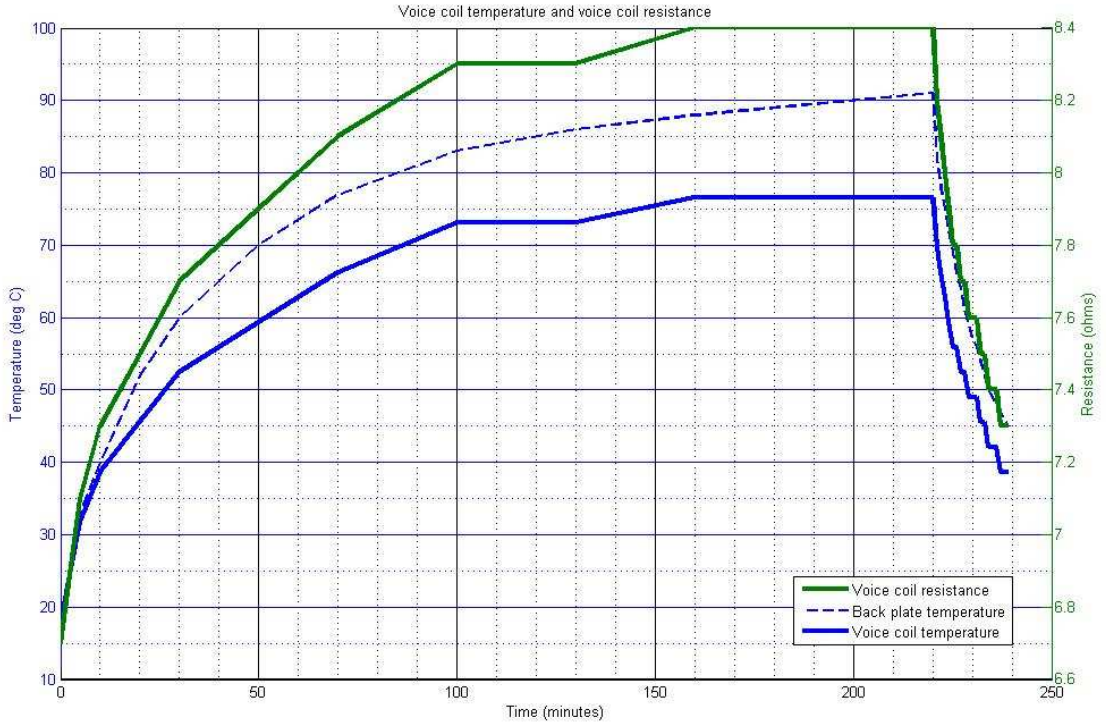

Figure 6.14: Temperature and DC resistance versus time plot (August 1, 2008 measurement data)

This plot illustrates the relationship between the back plate temperature and the voice coil temperature. The voice coil temperature is calculated directly from the DC resistance value, so it is expected that the two lines follow each other exactly. It can bee seen that both temperatures exhibit an approximately logarithmic rise over time. The discrete steps seen in the voice coil temperature and resistance lines can be attributed to the lack of measurement precision of the multimeter used in the measurements.

Evidence of heat transfer is clear as the back plate temperature quickly rises above the voice coil temperature after passing ten minutes of operation. After two hours of continuous operation there is a 15 °C temperature difference between the two. This shows that this driver was designed with adequate heat transfer mechanisms. The heat has been drawn out of the voice coil and into the surrounding structure. It can be expected that over time the

temperature difference would continue to rise until the structure reaches equilibrium (heat in = heat out) [2].

At 220 minutes into the testing, the white noise signal was turned off with new measurements now taken every minute. Again, the efficient heat transfer in the driver is visible as the temperature drops almost 40 °C over only twenty minutes. As the temperature gets lower the rate of temperature decrease lessens indicating that while the driver can quickly dissipate heat when experiencing high temperature levels, at lower temperature levels the voice coil is slower to cool.

In the loudspeaker measurements, the voice coil started at 18 °C (room temperature). The back plate temperature measurement reached a maximum at 91 °C, corresponding to a voice coil temperature of 76 °C (Equation 4.21). The majority of the data analysis will involve comparing the measurements at the two temperature extremes. Additional analysis will attempt to discover a pattern of change for the frequency response as the temperature changes.

There are data errors present at a few measurement points. This is due to the computer's lag time in taking quick measurements from the sound card. This would occasionally result in an MLS measurement being inaccurate. No errors occurred with any sweep measurements, therefore even when lacking a valid MLS measurement at a given temperature, there always exists a valid sweep measurement. These two measurements were used together to help validate the results, but also can help when one of the measurement types fails.

Due to the possibility of measurement error, it was important to first compare the MLS and sweep measurements for each polar position for the key data (temperature extremes) to ensure both are valid (**Figures 6.15, 6.16, 6.17, 6.18**).

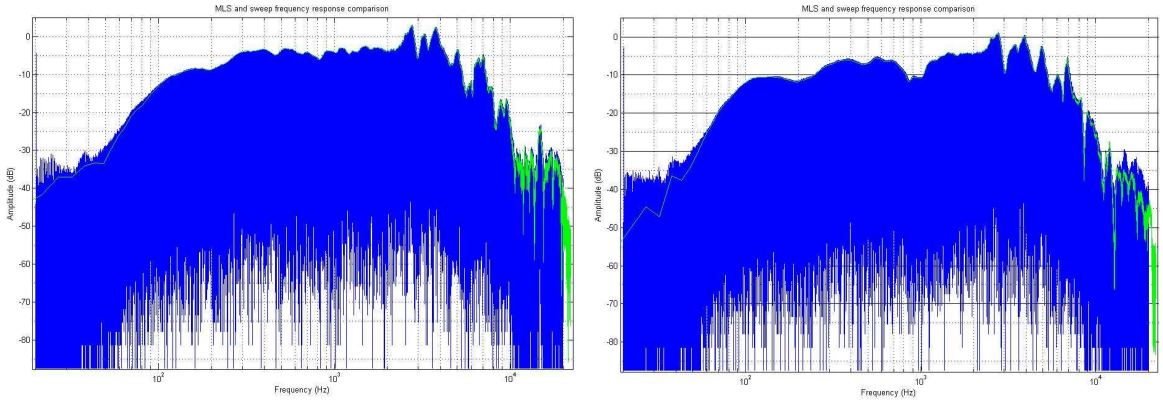

Figure 6.15: 0° MLS and sweep compare @ 18 °C (left) and 91 °C (right)

(MLS = green, sweep = blue)

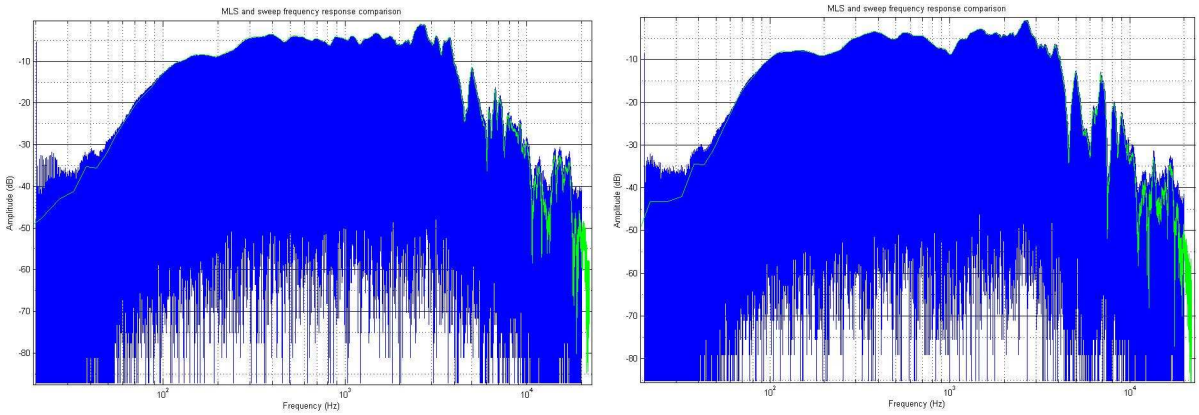

Figure 6.16: 30° MLS and sweep compare @ 18 °C (left) and 91 °C (right)

(MLS = green, sweep = blue)

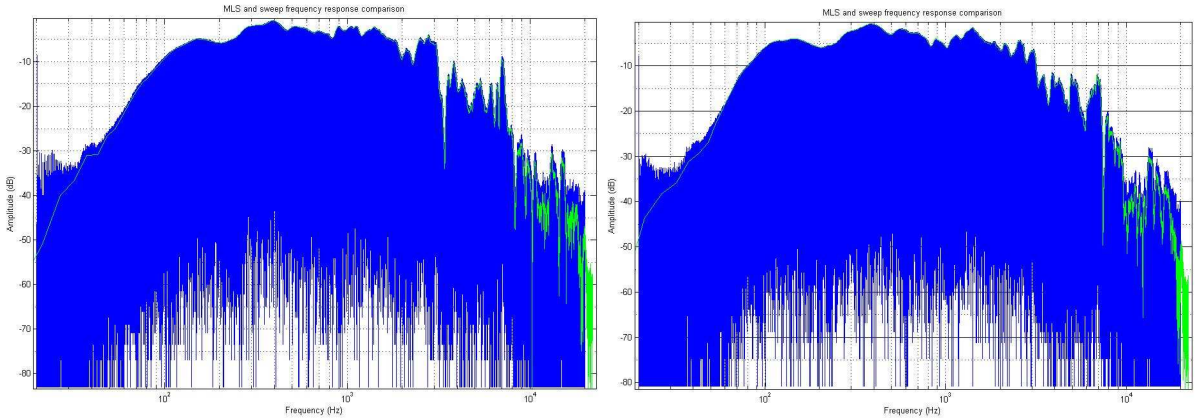

Figure 6.17: 60° MLS and sweep compare @ 18 °C (left) and 91 °C (right)

(MLS = green, sweep = blue)

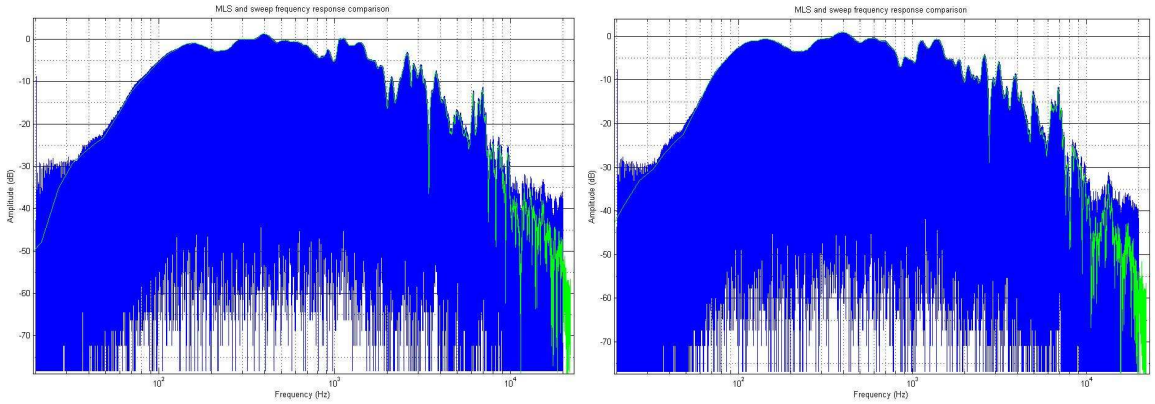

Figure 6.18: 90° MLS and sweep compare @ 18 °C (left) and 91 °C (right) (MLS = green, sweep = blue)

The above figures confirm that the MLS and sweep measurements line up closely for all polar positions. This will allow for the use of both measurements in data analysis for these temperature levels. The 0° polar position measurements can be compared to the manufacturer's advertised frequency response plot (**Figure 6.19**).

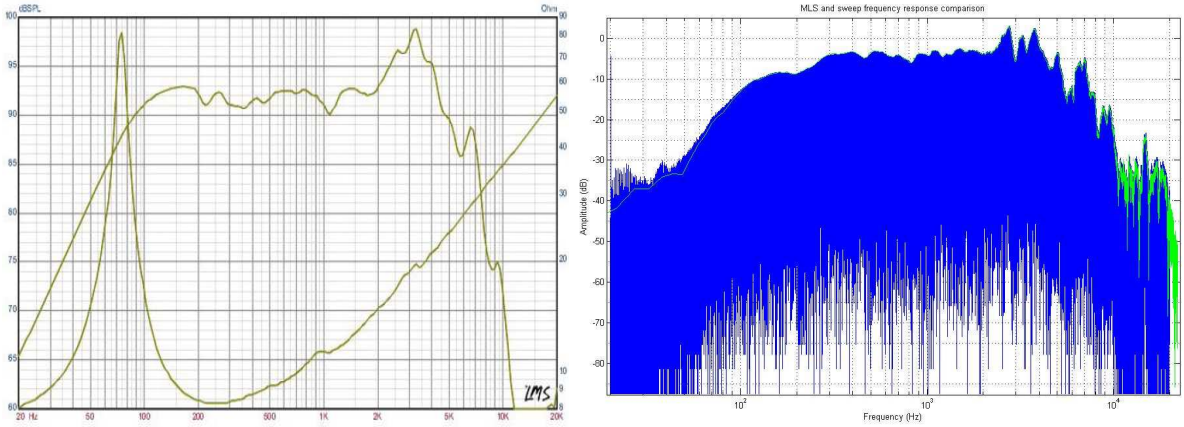

Figure 6.19: Frequency response plots for the Sovereign 8-125 driver (left) [14] and the measured driver frequency response (in enclosure) at room temperature (right)

The measured frequency response plot (on-axis at room temperature) lines up very nicely with the manufacturer's frequency response chart. Differences are due to the driver being mounted in the enclosure [16].

7.1 Maximum length sequences

The MLS measurements provide very precise frequency response data. In this case, the amplitude for each measurement is relative to only within each measurement. In other words, one can't use the MLS amplitudes to directly compare a measurement taken at 0 degrees

(perfectly on-axis) and at 90 degrees off-axis. This is due to normalization that occurs within the software.

The first comparison made was from 0 degrees (perfectly on-axis) measurements using data points corresponding to a back plate temperature of 18 °C and 91 °C (**Figure 6.20**).

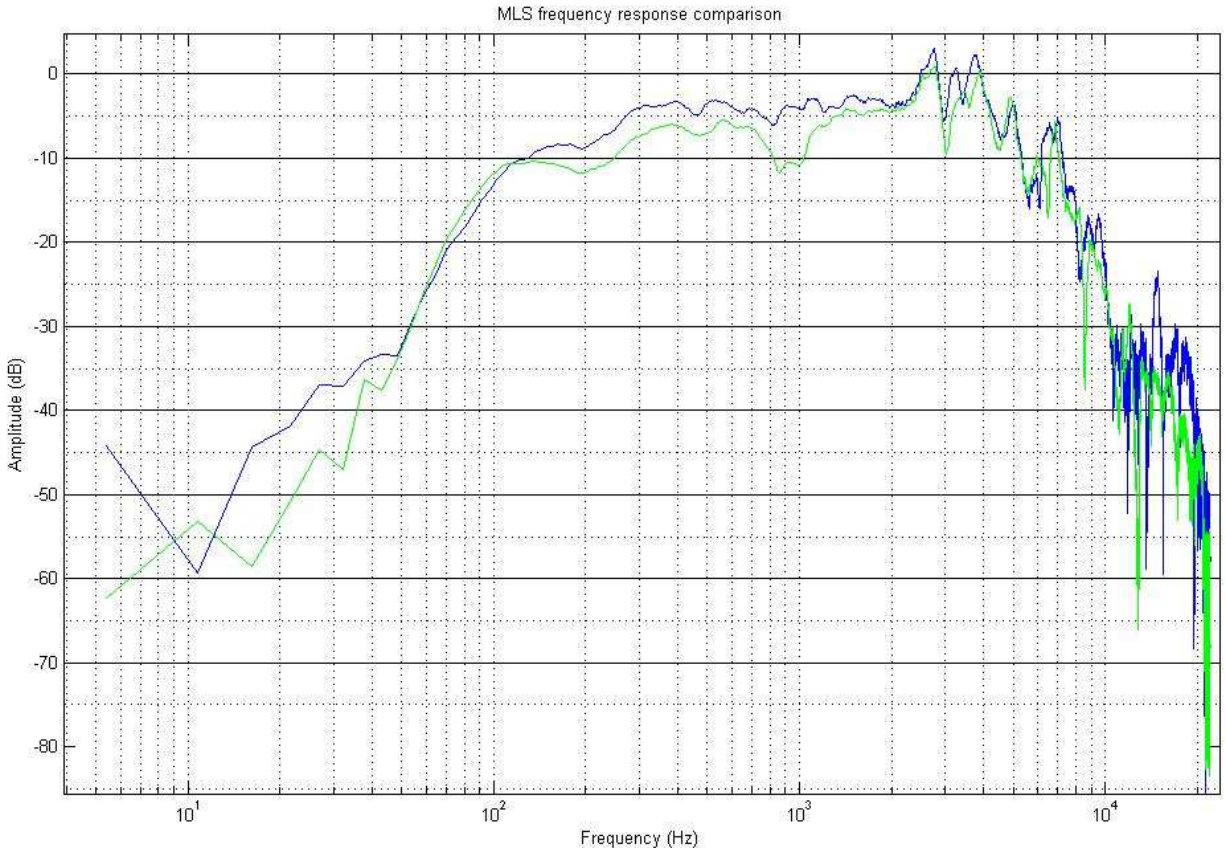

Figure 6.20: On-axis MLS comparison (18 °C = blue, 91 °C = green)

This comparison shows three separate frequency ranges exhibiting a decrease in amplitude with a rise in voice coil temperature. First is the lower frequency range of 0 – 50 Hz. The simulations performed in Chapter 5 did not show any expected drop at low frequencies since **Figure 5.2** shows little or no loss of efficiency for the frequencies below the resonant frequency. The drop seen in **Figure 6.20** is most likely due to the lack of precision of the MLS at very low frequencies. Analysis of the sweep measurements should show that this drop is not present.

An exception to this low frequency behavior is centered around 110 Hz. This behavior was shown in the loudspeaker simulation in Chapter 5 (**Figure 5.4**). An explanation for this may be that the boosted range is very close to the loudspeaker's resonant frequency of 90 Hz. 110 Hz is close to the starting point of a maximally flat response in the simulation. As the voice

coil temperature increases, the increased DC voice coil resistance may cause the resonant frequency to show itself in the loudspeaker's response through a decrease in the total quality factor.

The second frequency range showing a decrease in amplitude is a high frequency range from 10 – 20 kHz. This is largely due to a decrease in the total stiffness of the system. While the suspension stiffness is unchanged with temperature, the enclosed air stiffness changes due the rise in internal air temperature. This results in a change in total stiffness, giving the decrease in high frequency amplitude since it is harder for the moving mechanism of the driver to spring back to equilibrium position when operating at high frequencies.

The third frequency range that is affected by the voice coil temperature is a mid range frequency band centered just under 1 kHz. This decrease is amplitude is more difficult to explain. Upon inspection of the equations presented in Chapter 4, this dip in amplitude could be due to the inner dimensions of the loudspeaker enclosure.

As in a rectangular room, there should exist normal modes in this loudspeaker enclosure of dimensions 50 x 33 x 23 cm. These modes can be calculated using a simple equation that takes the dimensions and the speed of sound in air into account (**Table 6.1**) [16].

$$f = \frac{c}{2}\sqrt{(\frac{N_x}{l_x})^2 + (\frac{N_y}{l_y})^2 + (\frac{N_z}{l_z})^2} \tag{6.13}$$

Where,

f = normal mode frequency (Hz)

c = speed of sound in air (343.371 m/s @ 20 °C, 360.513 m/s @ 50 °C)

l_x = height of the enclosure (50 cm)

l_y = width of the enclosure (33 cm)

l_z = depth of the enclosure (23 cm)

N_x, N_y, N_z = mode labels (0, 1, 2, 3, …)

The enclosed air temperature was not directly measured, so an estimate had to be made by observing a clear frequency shift around 3.8 kHz. Through (6.13) a mode was found to be located at 3.748 kHz at 20 °C which would rise to 3.935 kHz at 50 °C. This shift lines up nicely with the noticeable frequency shift in the generated spectrogram (**Figure 6.20**). With this observation, the estimated maximum internal air temperature is 50 °C. Judging from the

spectrogram, the air temperature does not seem to rise linearly, but since only the minimum and maximum temperatures are concerned, the shift can be calculated as linear.

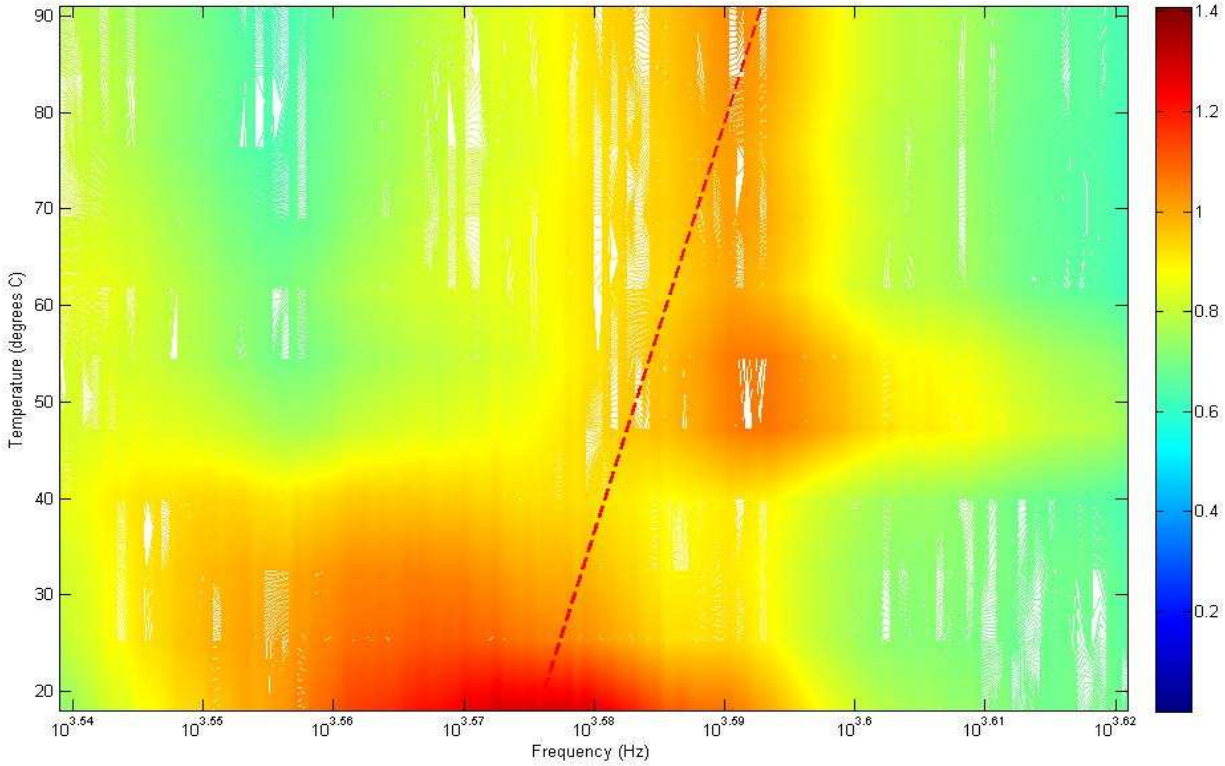

Figure 6.20: Spectrogram used for air temperature estimate (red line = modal shift)

N_x	N_y	N_z	**Mode Type**	**Frequency @ 20 °C**	**Frequency @ 50 °C**
1	0	0	Axial	343 Hz	361 Hz
0	1	0	Axial	520 Hz	546 Hz
1	1	0	Tangential	623 Hz	655 Hz
2	0	0	Axial	687 Hz	721 Hz
0	0	1	Axial	747 Hz	784 Hz
1	0	1	Tangential	822 Hz	863 Hz
2	1	0	Tangential	862 Hz	905 Hz
0	1	1	Tangential	910 Hz	955 Hz
1	1	1	Oblique	973 Hz	1.021 kHz
2	0	1	Tangential	1.014 kHz	1.065 kHz
0	2	0	Axial	1.041 kHz	1.093 kHz
2	1	1	Oblique	1.140 kHz	1.197 kHz
0	2	1	Tangential	1.281 kHz	1.344 kHz
1	2	1	Oblique	1.326 kHz	1.392 kHz
2	2	1	Oblique	1.453 kHz	1.526 kHz
0	0	2	Axial	1.493 kHz	1.568 kHz

Table 6.1: First 16 normal modes of the loudspeaker enclosure

There appears to be a concentration of modes around the 600 Hz to 1.2 kHz area which is exactly where the mid-range drop in response occurs (**Figure 6.21**). Note that the modes will shift upwards as the temperature of the enclosed air increases [16]. A shift from 20 °C to 50 °C will result in the frequencies shifting up by 4.99% (**Figure 6.22, 6.23 & 6.24; Table 6.1**).

This mid-range dip is described in [17] as a result of these internal resonant modes. Since the driver is located in the x-y plane and its motion is parallel to the z axis, the most important modes will be those that also have motion parallel to the z axis. With this in mind, the most important modes should be first, those only along the z-axis: (0, 0, 1) and (0, 0, 2). (0, 0, 2) is out of the range we are focusing on, but (0, 0, 1) is located at 747 Hz at room temperature. **Figure 6.22** shows this mode to be located in the first half of the mid-range dip. With the air temperature increased to 50 °C, this mode rises to 784 Hz which is again in the first half of the mid-range dip (**Figure 6.23**).

A second type of mode that can play a large role in this mid-range dip is the type that has motion both in the direction of the driver movement and also along the x axis (up/down direction). This would correspond to the (1, 0, 1) mode which is located at 822 Hz at room temperature and at 863 Hz at 50 °C. This mode is located at the point where the mid-range dip is at its maximum at both temperatures (**Figures 6.22 & 6.23**). The strong effect of this mode is due to the driver being in the lower half of the enclosure. Along this diagonal, there will be a full wavelength within the enclosure [16]. This means that the driver will encounter only half the wave at a time so it will either be pushing or pulling the driver at any one time (but never doing both).

All other modes are not expected to have as significant an effect on the dip because they can be pulling and pushing the driver at the same time. This doesn't allow for a strong coupling between the driver motion and the wave motion. In general, the modes of (0, 0, z) and (1, 0, z) would have the strongest effect, but where $z > 1$, the frequency is out of the mid range dip area that is described in [17], allowing us to focus on modes with $z = 1$.

An important note is that the enclosure is not perfectly rectangular. The important modes discussed above occur between parallel walls of the enclosure, but other walls are not parallel. Also, the inside of the enclosure has a supporting structure which further

complicates determining the modes. For this project, the simple rectangular dimensions calculation was used (6.13) and it must be stressed that this will not give the exact internal modes of this enclosure. It does give close approximations, though, which are seen as the calculated modes line up nicely with the experimental data (**Figures 6.21, 6.22 & 6.23**).

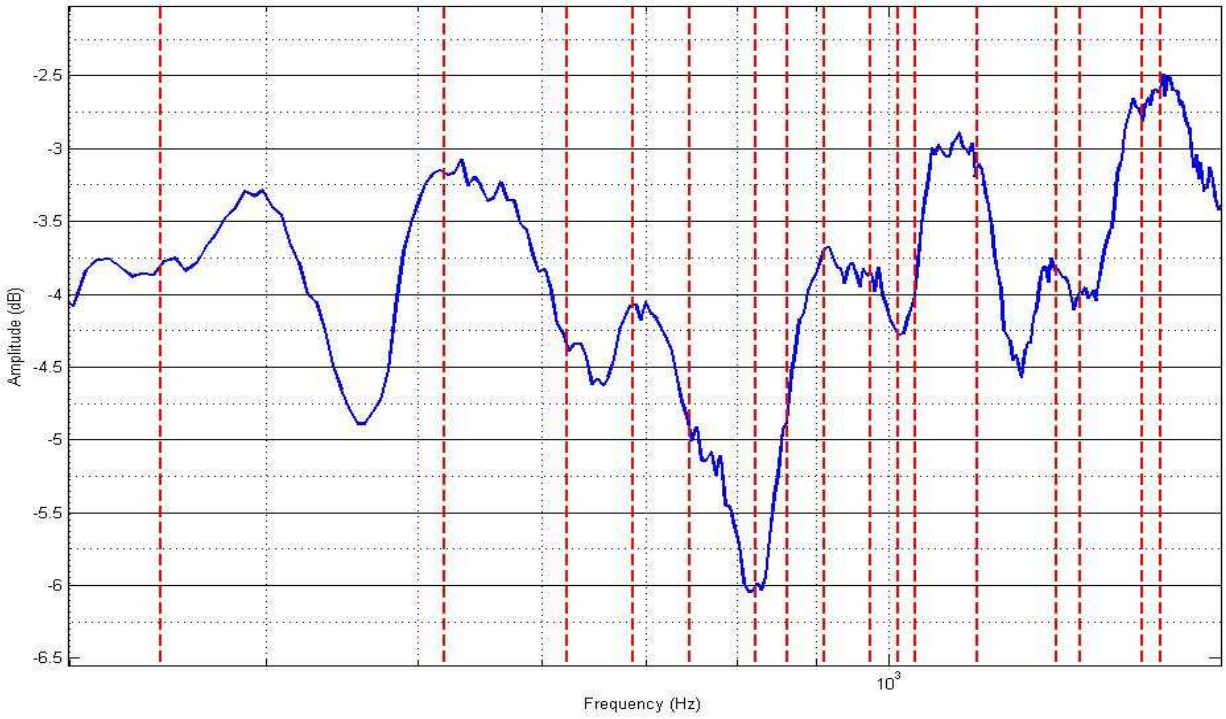

Figure 6.21: Examination of resonant modes in the on-axis frequency response @ 20 °C

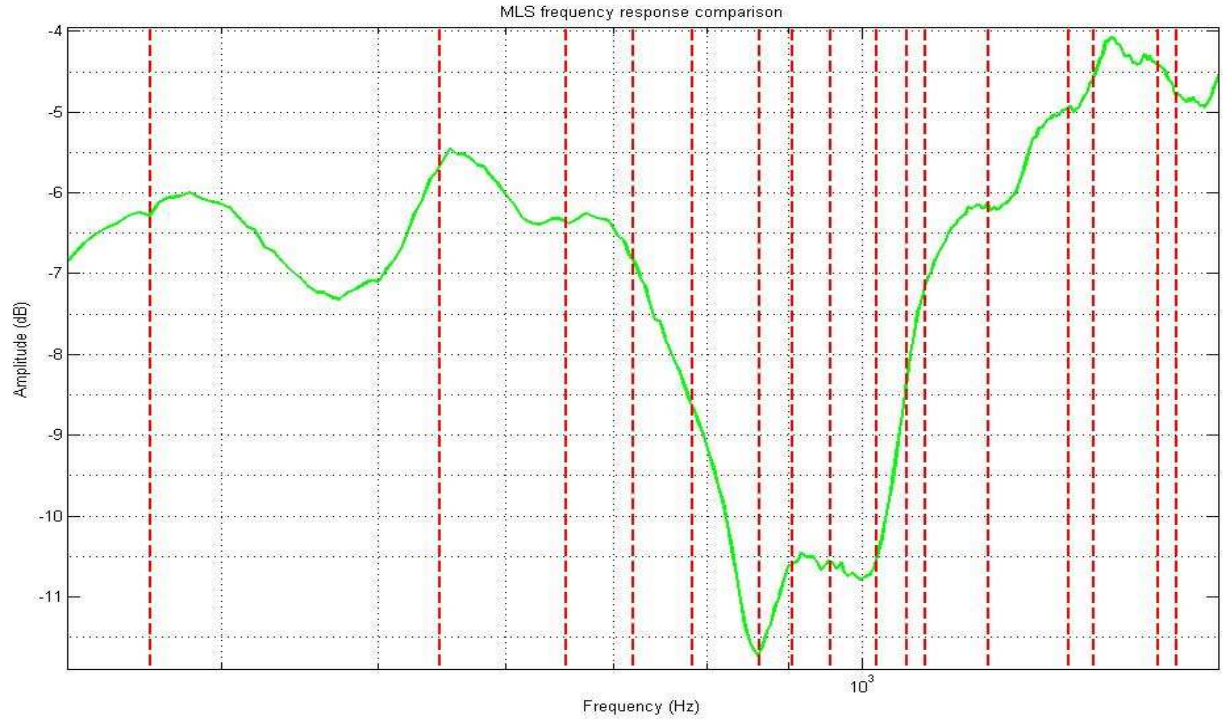

Figure 6.22: Examination of resonant modes in the on-axis frequency response @ 50 °C

Through close examination of the MLS measurements, the mid-range dip is visible at room temperature, but is far less in amplitude than when at heightened temperatures. It is possible that as the temperature rises, the internal pressure between the driver and the air inside the enclosure becomes greater, resulting in the noticeable drop in response (**Figure 6.23**).

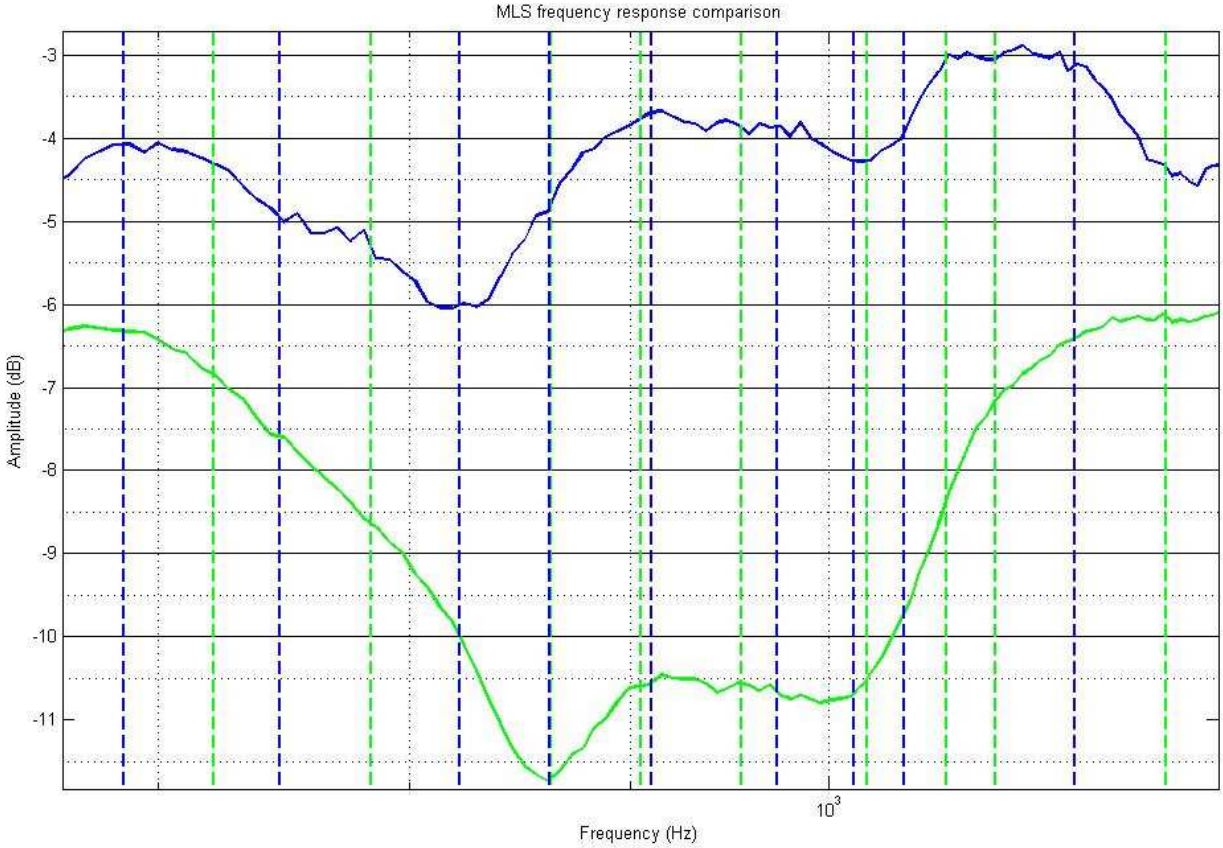

Figure 6.23: Comparison of resonant modes in the on-axis frequency response (blue = 20 °C, green = 60 °C)

With the decrease in amplitude due to voice coil temperature giving interesting results, it is important to examine if these effects are present (and to what extent) at off-axis measurement positions. The first position analyzed was 30 degrees off-axis (**Figure 6.24**). Nothing else was changed in the measurement procedure.

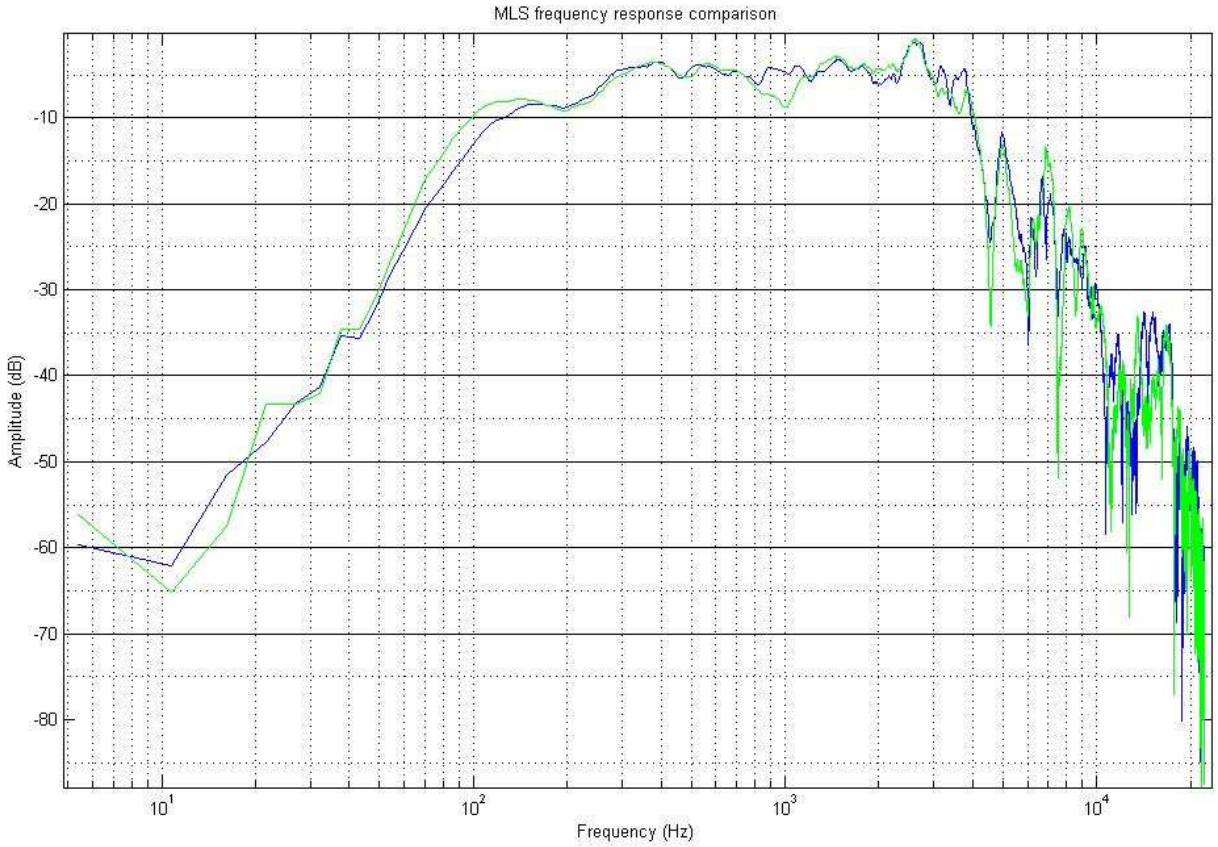

Figure 6.24: 30° off-axis MLS comparison (18 °C = blue, 91 °C = green)

The same decreases in amplitude over the three frequency ranges are still present at thirty degrees off-axis, but are less in magnitude. Again, a low frequency drop can be seen and this will be explored further in the sweep analysis. The high frequency response still decreases with temperature, but is less in extent that with the on-axis measurements.

The mid-range amplitude dip is again present. While the on-axis measurement showed a drop of around 6 dB at this point, at 30 degrees off-axis the drop appears to only be around 3 dB. The smaller drop at this position can be due to slight time delay between the arrival of the sounds on the nearer portion of the cone and the sounds on the distant portion of the cone. This can cause a phase problem, resulting in a decease in amplitude at the measurement point.

Continuing on with the analysis, the MLS measurements at 60 degrees off-axis were compared (**Figure 6.25**).

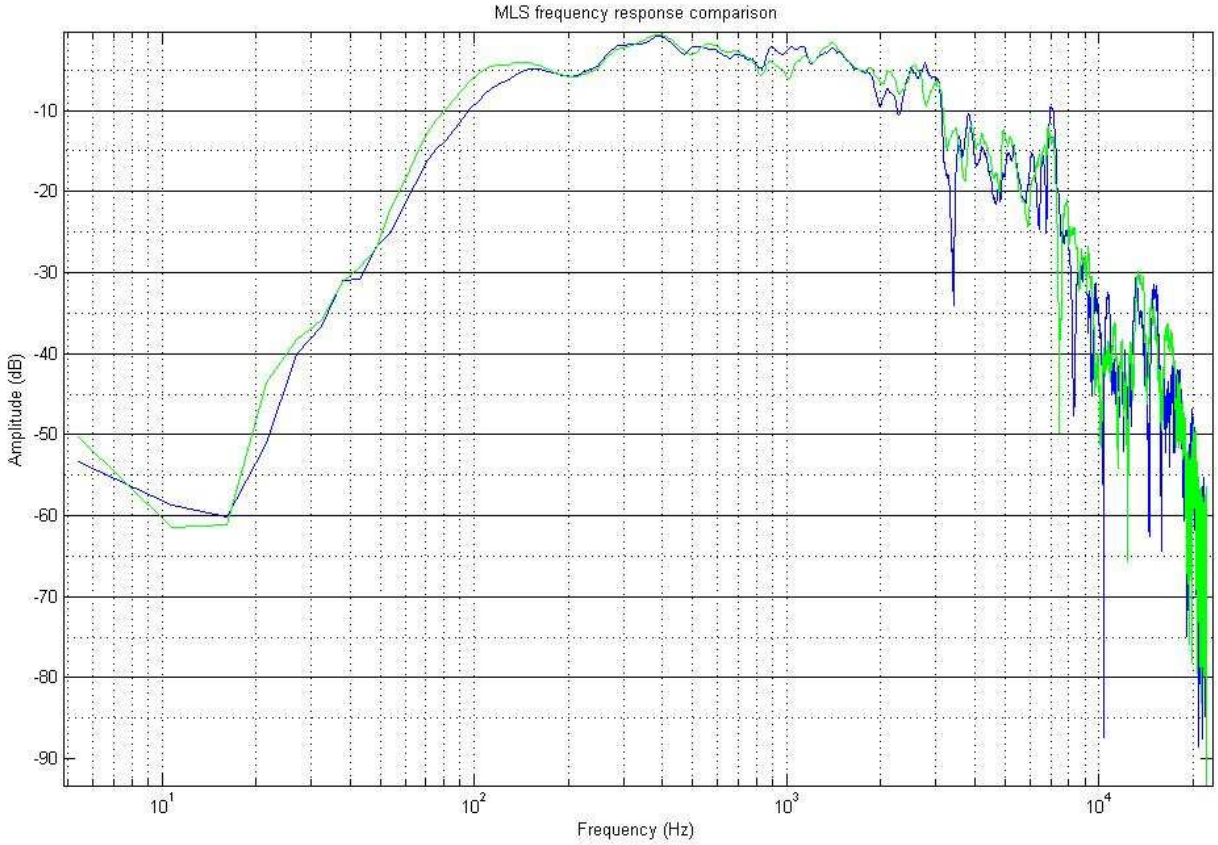

Figure 6.25: 60° off-axis MLS comparison (18 °C = blue, 91 °C = green)

This measurement set does not clearly exhibit a drop in amplitude for the low and high frequency ranges. This can be attributed to the time delay issue of the signal arriving at the microphone at slightly different times causing a phase issue. The boost around 110 Hz is still clearly visible, as expected from the simulations in Chapter 5.

Again, there is a clear dip in amplitude around 1 kHz, although this time around 2 dB in magnitude. This lessened magnitude can again be attributed to the phase issue, but it is a great enough drop to still be noticed.

Lastly, the 90 degree off-axis measurements were compared to one another (**Figure 6.26**). It would be expected that this comparison would follow the pattern already seen where the amplitude dips are less noticeable the more off-axis the measurement position.

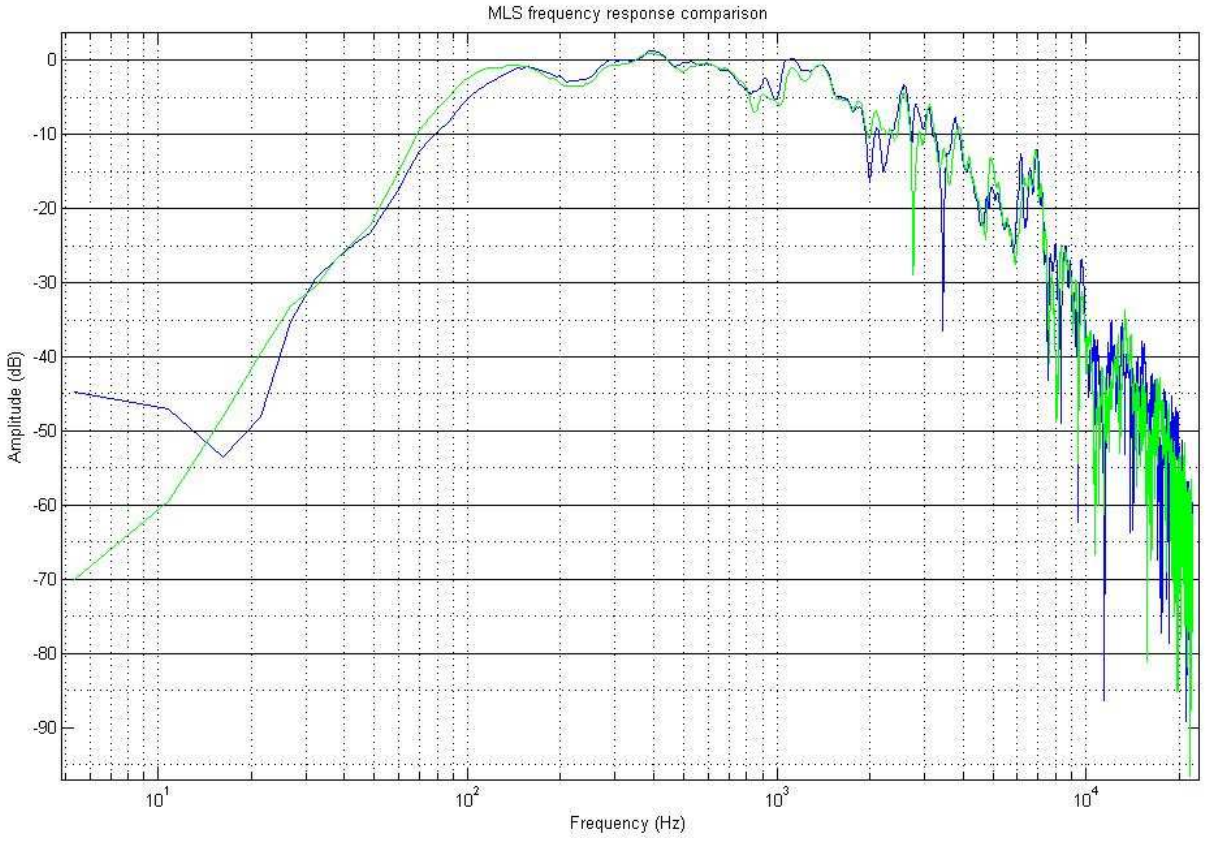

Figure 6.26: 90° off-axis MLS comparison (18 °C = blue, 91 °C = green)

This measurement comparison follows the established pattern of the previous comparisons. While the high frequency dip has disappeared, the mid-range dip and the boost around 110 Hz are still noticeable. One interesting observation is that this dip has now shifted slightly down in frequency. Now it is centered around 800 Hz. This may be due to phase issues for the higher frequencies in this range.

7.2 Sinus-logarithmic sweep

With the MLS measurements analyzed, the sweep measurements now can be used for two important tasks. First, they need to be able to verify what was found with the MLS data. If the same dips are observable as in the MLS data, the data can be considered valid and the analysis can move forward. Secondly, the sweep data provides a comparison possibility that the MLS data cannot. Since the sweep measurements never undergo normalization, the data from different measurement positions can be directly compared to determine the change in amplitude due to the measurement position.

First, the data will be compared to the MLS data (**Figures 6.27, 6.28, 6.29, 6.30**). If the plots are consistent with one another, the measurement analysis can move forward with full confidence of data validity.

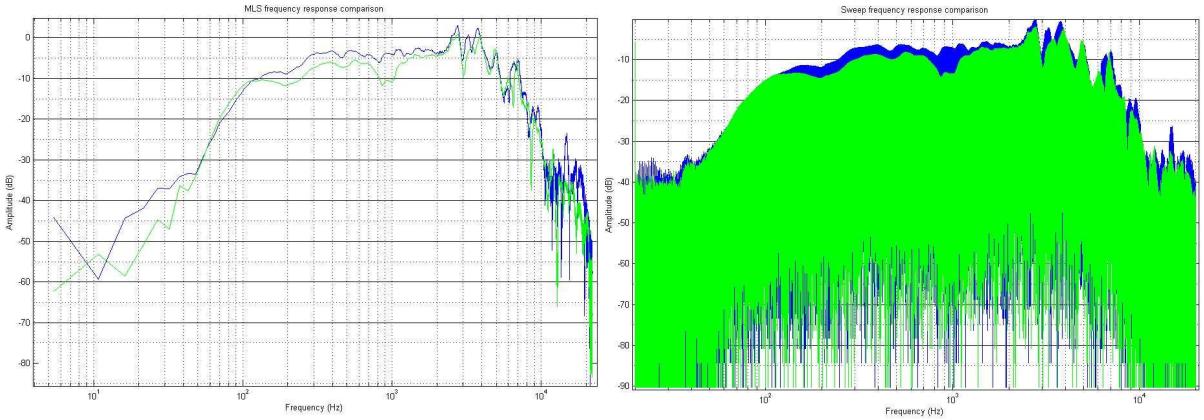

Figure 6.27: MLS (left) and sweep (right) data comparison on-axis
(18 °C = blue, 91 °C = green)

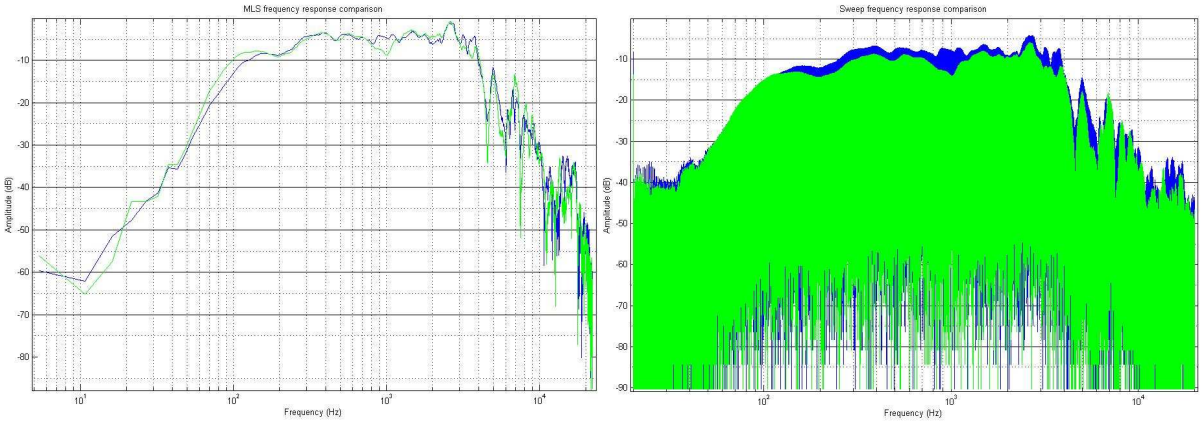

Figure 6.28: MLS (left) and sweep (right) data comparison @ 30° off-axis
(18 °C = blue, 91 °C = green)

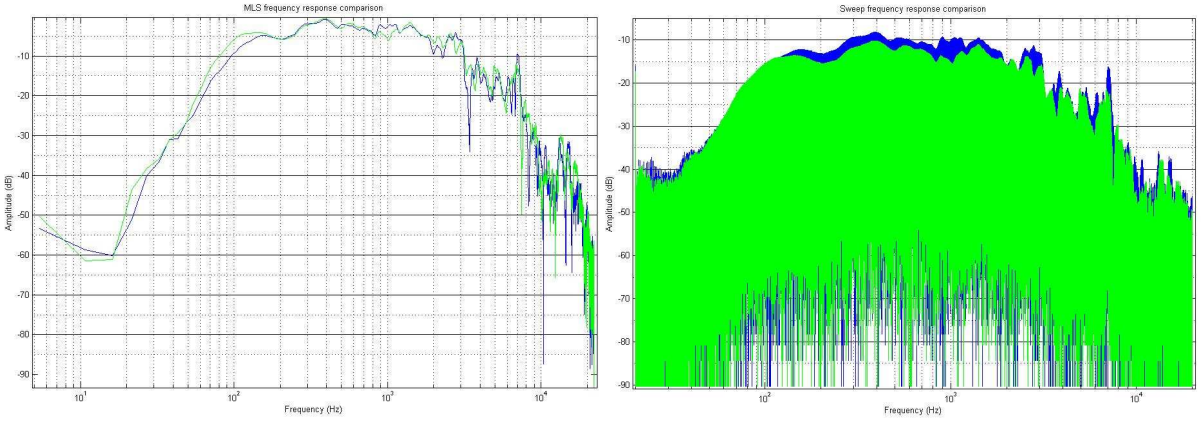

Figure 6.29: MLS (left) and sweep (right) data comparison @ 60° off-axis
(18 °C = blue, 91 °C = green)

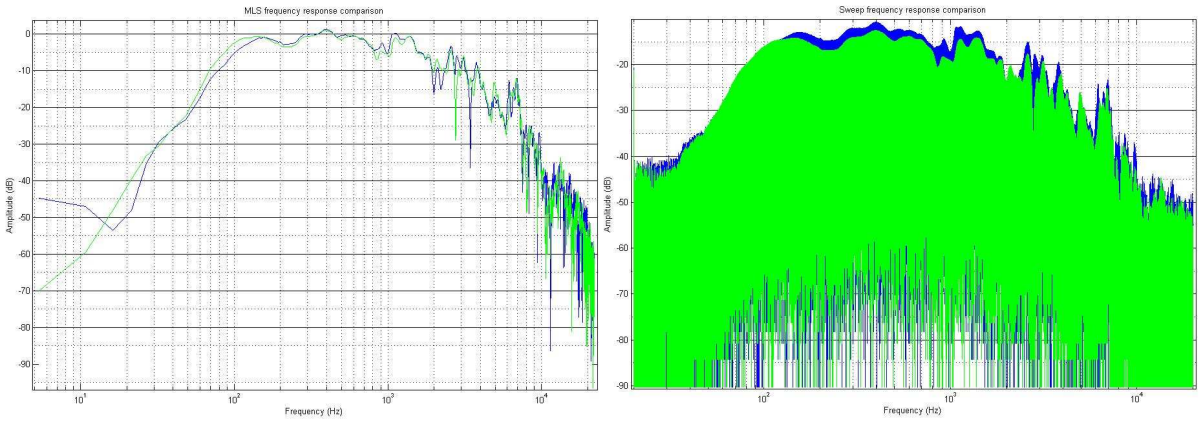

Figure 6.30: MLS (left) and sweep (right) data comparison @ 90° off-axis (18 °C = blue, 91 °C = green)

All measurements contain nearly identical frequency response dips. The only difference, as expected, is that the loss in low frequency response with temperature is not present in the sweep measurements. Since both the simulation results in Chapter 5 and the sweep measurements show no drop in low frequency response with temperature, the MLS data showing the drop can be attributed to a lack of accuracy of the MLS at low frequencies.

The sweep measurements can now be used to compare the frequency responses at the different measurement positions (**Figures 6.31, 6.32 & 6.33**). The comparisons will all be done with respect to the on-axis measurement.

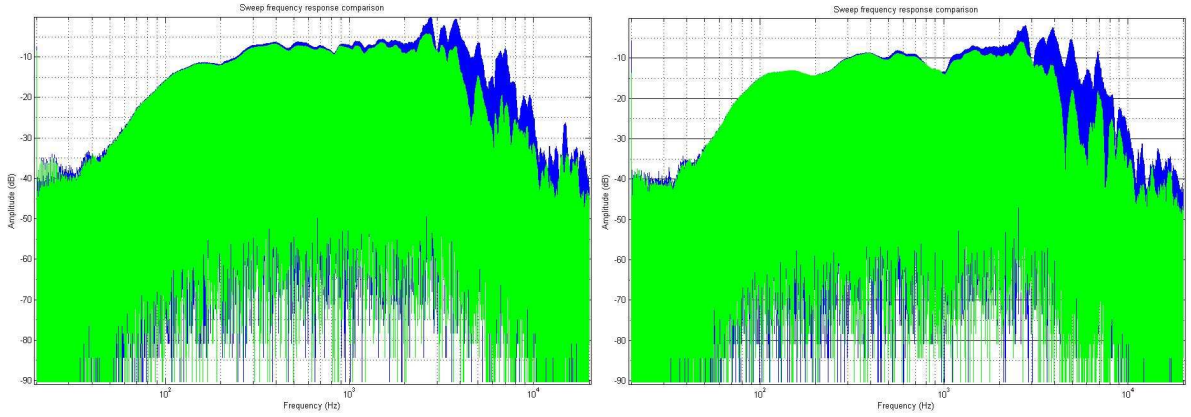

Figure 6.31: Comparison of 30° off-axis sweep measurement to on-axis sweep measurement @ 18 °C (left) & 91 °C (right) (on-axis = blue, off-axis = green)

In examining the on-axis and thirty degree off-axis measurement, it can be seen that the low frequency response is practically unchanged. As the frequency gets higher, there is a considerable decrease in amplitude. This is likely due to the above mentioned phase issues. Comparing the room temperature measurements to the heightened temperature

measurements, it is observable that both positions experience a similar change in frequency response, most notably around 1 kHz. Another visible (and expected) change in response due to temperature is the boost around 110 Hz. This is present at both measurement positions, helping to verify the simulation results. It appears that both measurement positions have experienced an amplitude decrease around 1 kHz of approximately equal magnitude. The existence of this relationship will be examined in the remaining two measurement position comparisons.

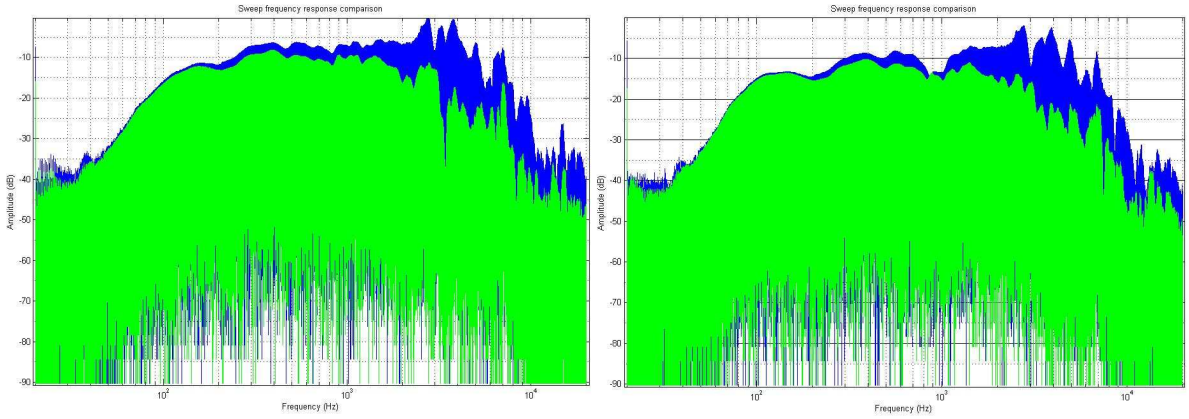

Figure 6.32: Comparison of 60° off-axis sweep measurement to on-axis sweep measurement @ 18 °C (left) & 91 °C (right) (on-axis = blue, off-axis = green)

Upon inspecting this comparison, the low frequency responses seem to still agree with one another at both measurement positions and voice coil temperature values. There appears to be even more of a high frequency loss due to the greater distance off axis. Also, the point at which the high frequency response begins to drop off is around 1.05 kHz where at thirty degrees off-axis it begins around 1.3 kHz. More importantly, is can be seen that the drop in amplitude around 1 kHz is now considerably less than for the on-axis measurement. This is consistent with the MLS analysis.

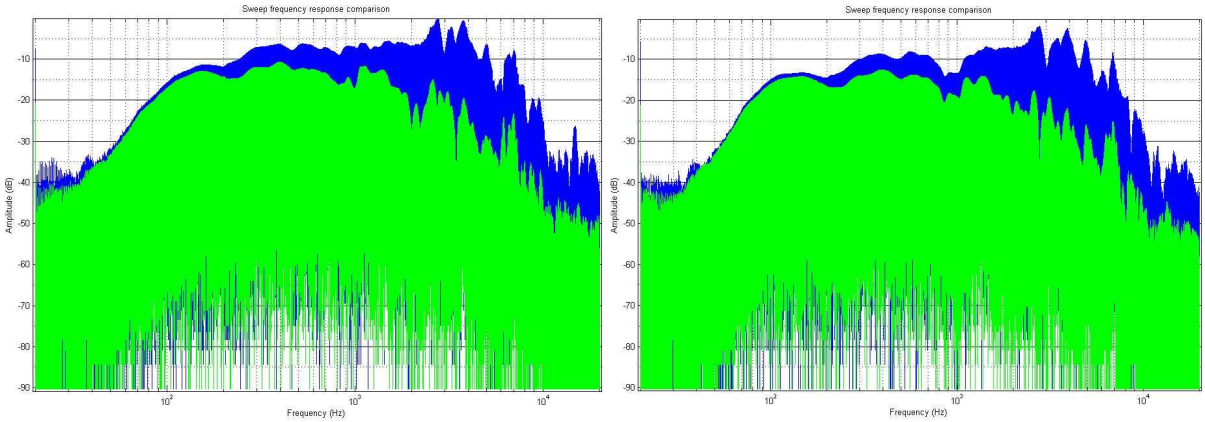

Figure 6.33: Comparison of 90° off-axis sweep measurement to on-axis sweep measurement @ 18 °C (left) & 91 °C (right) (on-axis = blue, off-axis = green)

The already noticeable trends in the change in frequency responses continue with the analysis of the ninety degree off axis measurements. Now, the high frequency drop off begins well below 1 kHz, around 400 Hz. The low frequency response still remains nearly unaltered due to the position change. This is because low frequencies have much longer wavelengths than the driver itself. This makes the time difference of signal arrival at the microphone almost trivial as phase differences will not be enough to cause a noticeable drop in amplitude [1].

The analysis of the sweep measurement gives two important results. First, it verifies the MLS data except for the low frequency drop. Secondly, the sweep comparison was performed between measurement positions, which was not possible with the MLS data, and shows that there is a correlation between the off-axis measurement position and the point of high frequency roll off. At thirty degrees off-axis the roll-off begins around 1.3 kHz while at ninety degrees off-axis the roll-off begins around 400 Hz. This means that the farther off-axis a listener is located, the more the high frequency will be reduced. This will result in a more muffled sound off-axis that is less than desirable in a high quality system that aims to cover a wide listening area. This loss in high frequency response is only heightened with increased voice coil temperature, but there doesn't appear to me more of a loss with temperature the farther off-axis the measurement position.

7.3 Further measurement analysis

The analysis software includes a function to generate three dimensional plots of the frequency response versus time for one measurement position at a time. A drawback of this method is that it is processor intensive. This means that, realistically, only the small sized MLS data collections could be utilized for this process. The twenty second sweep data would be far too large to plot without running out of memory in MATLAB.

As stated earlier, there exist a few MLS data errors. These occur at the on-axis position at 60 °C and 70 °C. To avoid an inaccurate plot, data was taken from measurements on a different day, but under identical conditions. The temperature and DC voice coil inductance are identical for the bad data and the replacement data, allowing the plot to be as accurate as possible, without error.

The resulting plots (**Figures 6.34, 6.35, 6.36 & 6.37**) should exhibit the observed characteristics from the previously performed analysis. The new plots will give a more

detailed picture of how the frequency response changes over time in an easy to read format. Since the loudspeaker response is roughly flat over the mid-range frequency spectrum, the logarithmic scaled plots may be difficult to read when examining for response change as the temperature increases. In response to this problem, linear scaled plots were also generated to help in the analysis process.

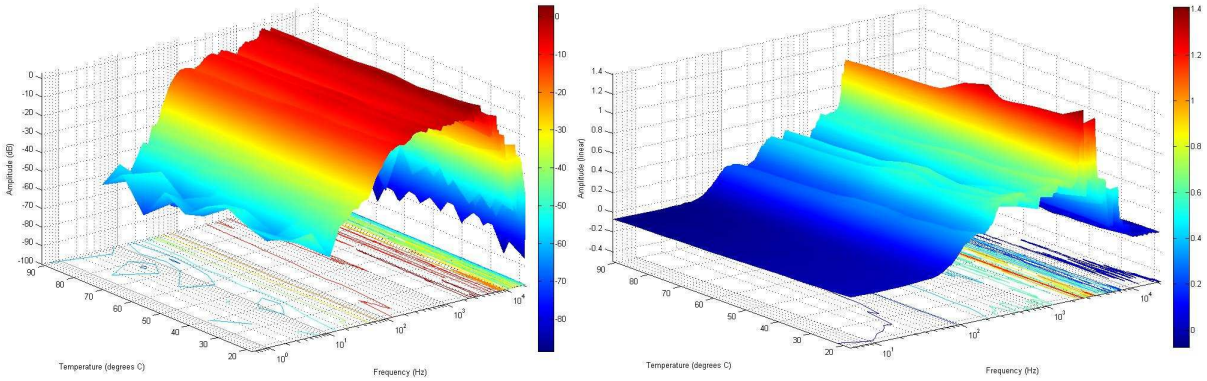

Figure 6.34: On-axis frequency response versus voice coil temperature (left = logarithmic, right = linear)

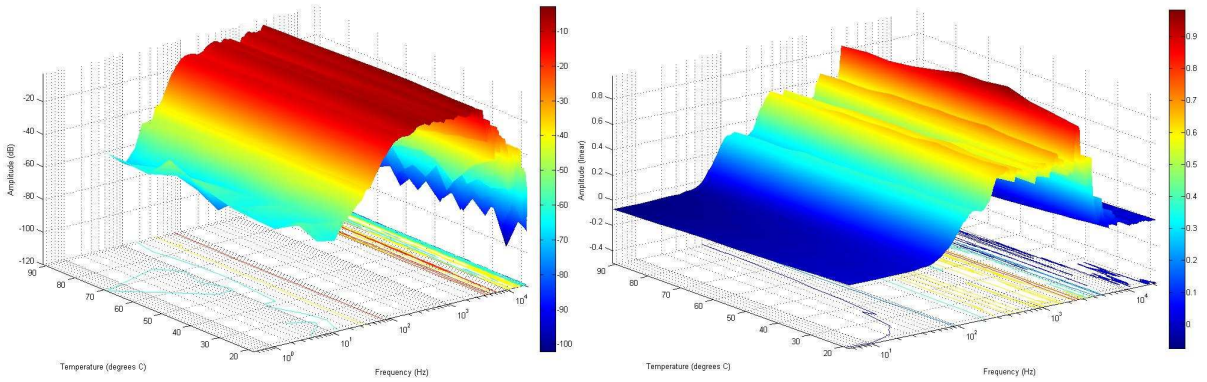

Figure 6.35: 30 ° off-axis frequency response versus voice coil temperature (left = logarithmic, right = linear)

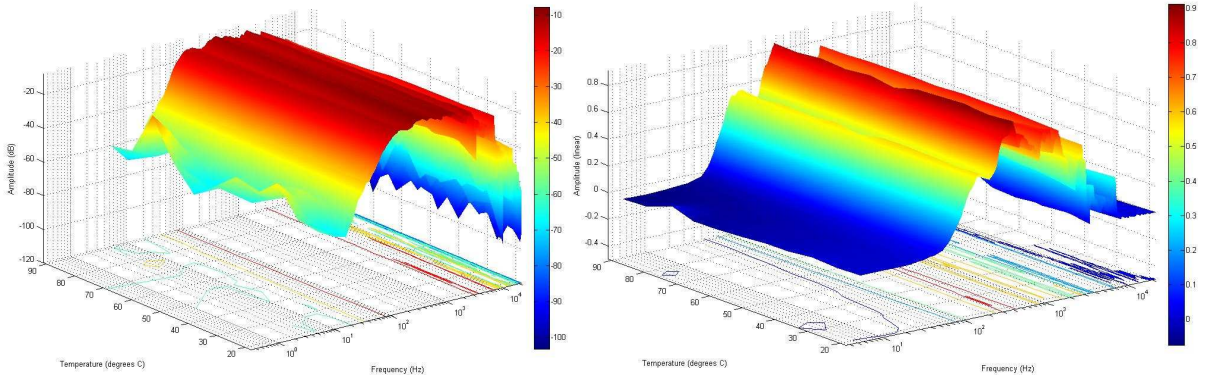

Figure 6.36: 60 ° off-axis frequency response versus voice coil temperature (left = logarithmic, right = linear)

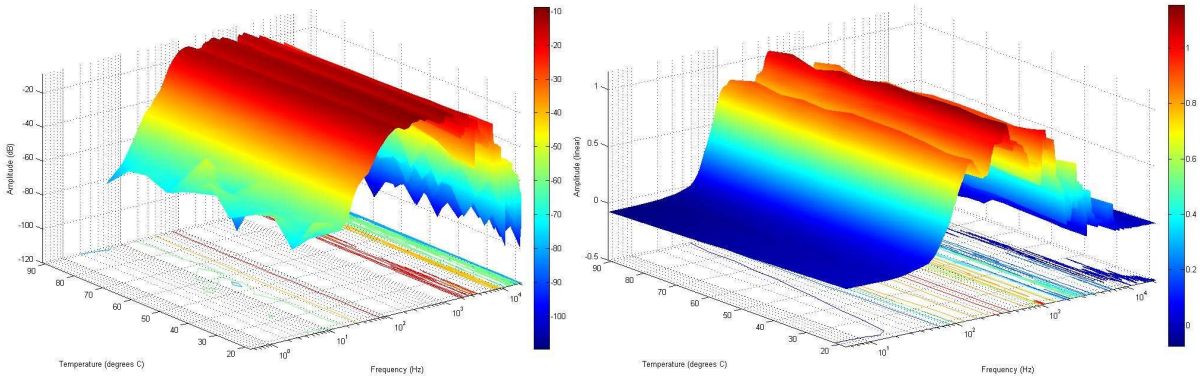

Figure 6.37: 90 ° off-axis frequency response versus voice coil temperature (left = logarithmic, right = linear)

These plots show clear dips around the peak amplitude values. Also, under close inspection, each plot shows the amplitude dip centered around 1 kHz to increase with temperature. In some cases for the off-axis measurements, certain frequency ranges rise for a certain temperature range. This again is likely due to the phase issues which affect the frequency response, primarily at higher frequencies where the wavelength is much less than the driver's diameter [1].

The three dimensional plots were then rotated to give a two-dimensional spectrogram view of the data. This will give the clearest idea of what happens to the frequency response due to the increased voice coil temperature and will also allow for further examination of the modal shifting effects on the response.

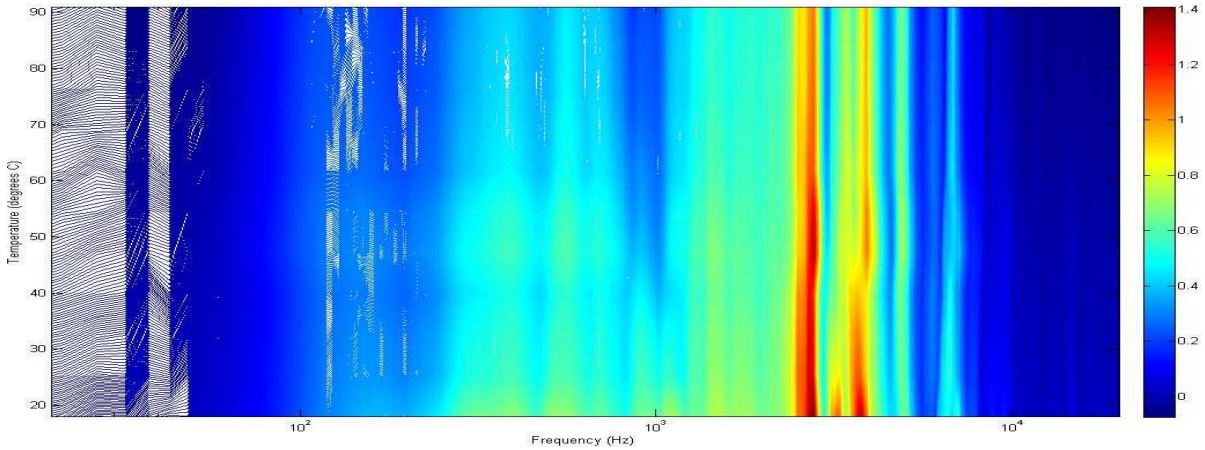

Figure 6.38: On-axis frequency response vs. temperature

The on-axis measurement data confirms the trends already noticed in previous data analysis. There is a mid-range drop over the temperature range. There is also a large drop around 12 kHz with additional drops being present for frequencies above 10 kHz. This shows that the voice coil temperature has a significant effect on high frequency performance. Low

frequency response, on the other hand, appears to be only slightly affected. The visible shifts in peak amplitudes can be attributed to the increase of the speed of sound in the enclosed air [16] as discussed earlier. It should be expected that all frequencies on the plot exhibit an upward shift in value as temperature increases (**Figures 6.39 & 6.40**).

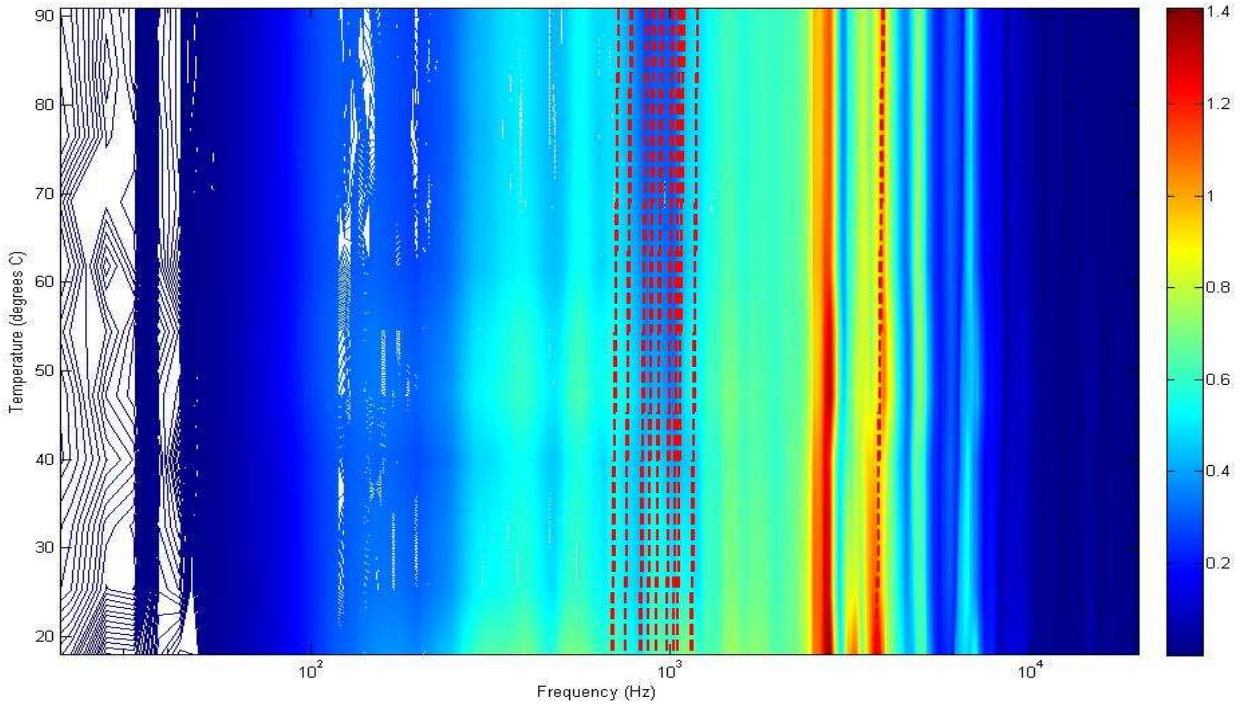

Figure 6.39: On-axis spectrogram with modal shifts due to temperature (red lines)

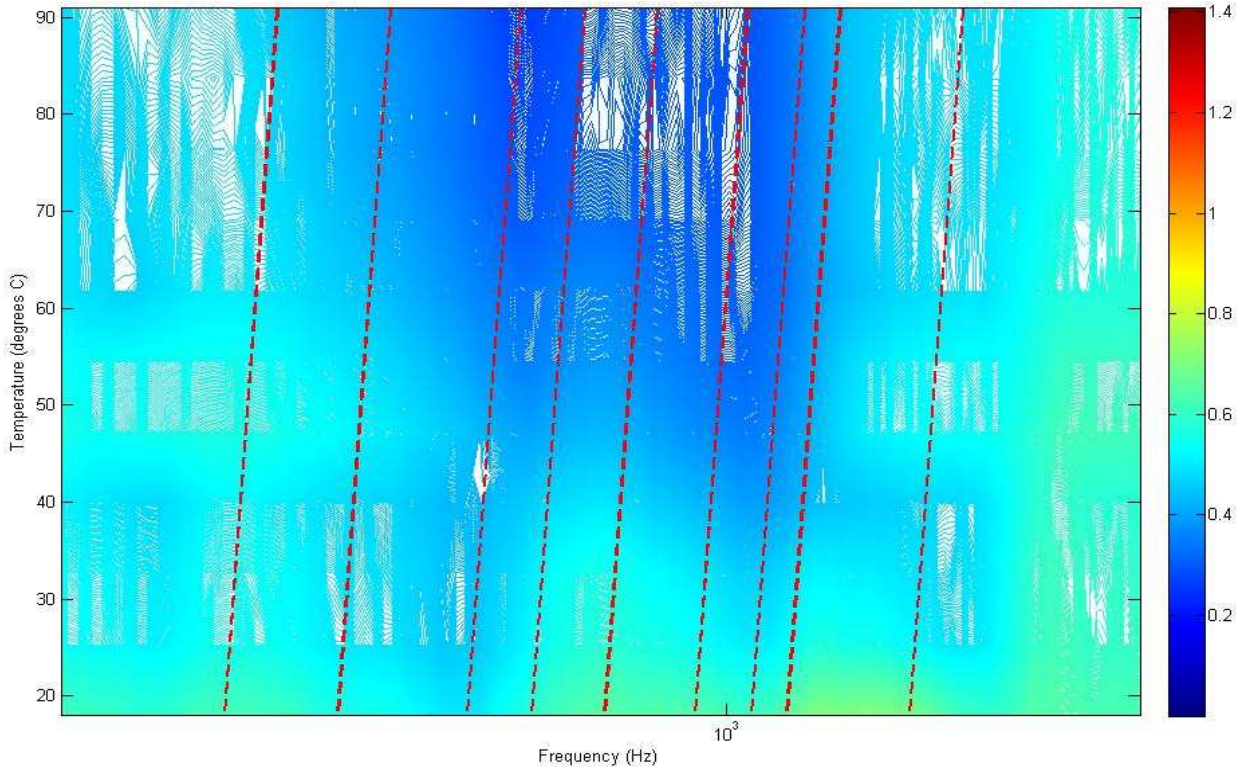

Figure 6.40: On-axis spectrogram with modal shifts (red lines) around 1 kHz

A very interesting shift of modes can be seen around the 1 kHz area as temperature increases (**Figure 6.40**). These modes seem to shift directly into the range exhibiting the loss in mid-range response. This serves to strengthen the argument that these enclosure resonant modes play a role in the loudspeaker's frequency response as the temperature rises.

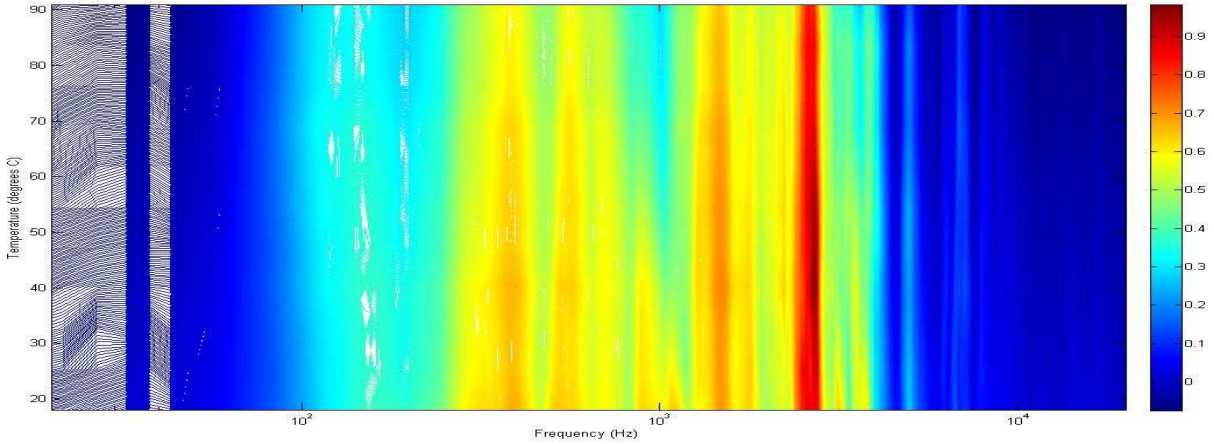

Figure 6.41: 30° off-axis frequency response vs. temperature

Similar patterns exist at thirty degrees off-axis. Again, a drop in response around 1 kHz is noticeable. Above 10 kHz, there is a significant drop in frequency response. At this measurement location the two highest drops occur around 15 kHz and 17 kHz. As with the on-axis measurements, the low frequency range is mostly unaffected by the temperature increase.

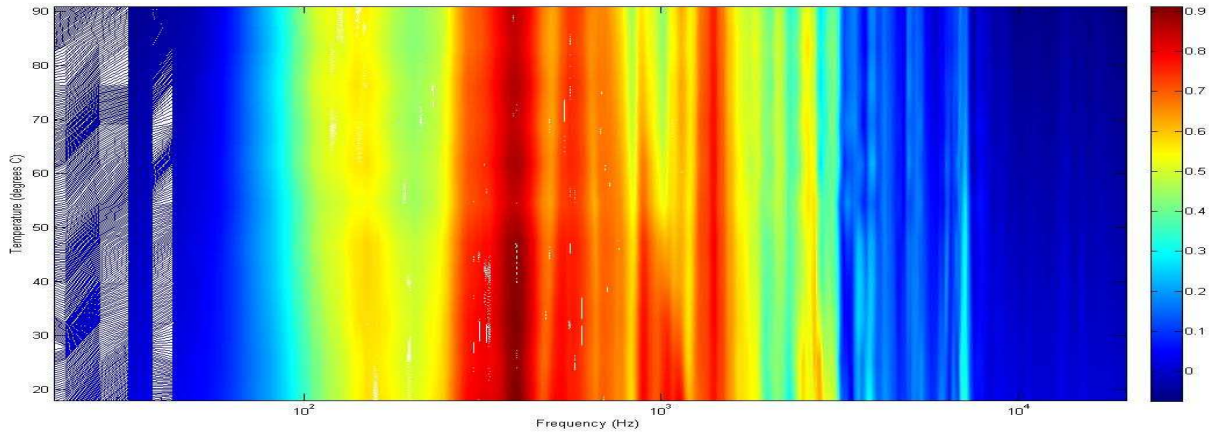

Figure 6.42: 60° off-axis frequency response vs. temperature

At a measurement position of 60 degrees off-axis, the high frequency response pattern begins to change. Now the response starts to drop off due to temperature starting around 7 kHz. The most significant drops now occur around 10 kHz while 15 kHz experiences less of a drop. The drop around 1 kHz is still present at this measurement position.

The expected increase in amplitude around 110 Hz becomes very visible at this measurement position. While the rest of the spectrum is experiencing a decrease in amplitude, this area is experiencing an increase in amplitude. This is important to notice, because otherwise it would appear that the upwards shift in frequency due to the air temperature has been reversed. With the knowledge of the increased response at this frequency, this behavior can be understood.

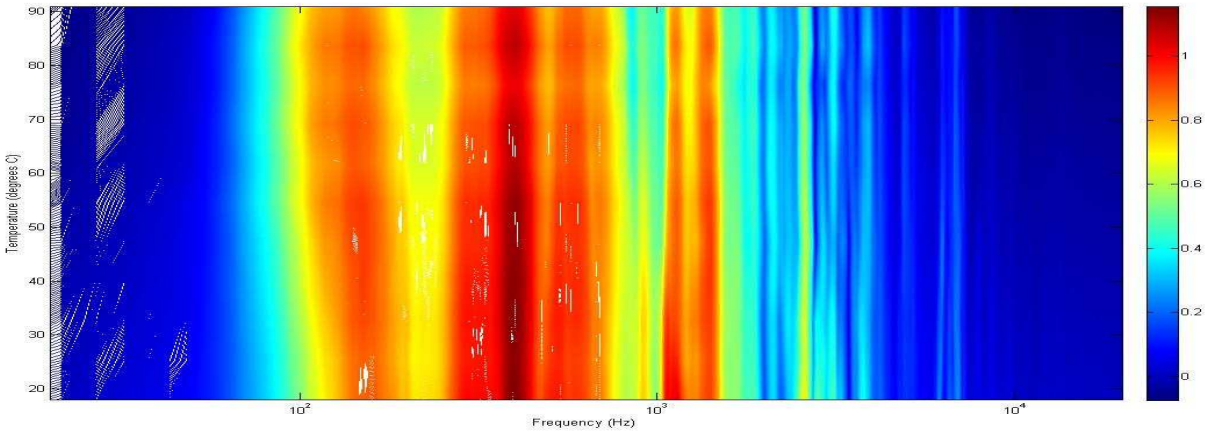

Figure 6.43: 90° off-axis frequency response vs. temperature

At ninety degrees off-axis, the frequency response over the temperature range exhibits similar trends as with sixty degrees off-axis. The high frequency response drop now begins around 6 kHz. The plot shows a drop present around just under 1 kHz which is consistent with previous observations. Even at ninety degrees off-axis, the low frequency range is largely unaffected by the temperature increase of the voice coil except for the now clearly visible increase around 100 Hz.

7.4 Sources of error

As mentioned earlier, certain MLS measurements did not properly line up with the input signals due to errors during data acquisition. If left unchecked, the invalid data would appear on the three dimensional plots as strange spikes (**Figure 6.44**). This was addressed by replacing the invalid data with data taken under similar conditions whenever possible.

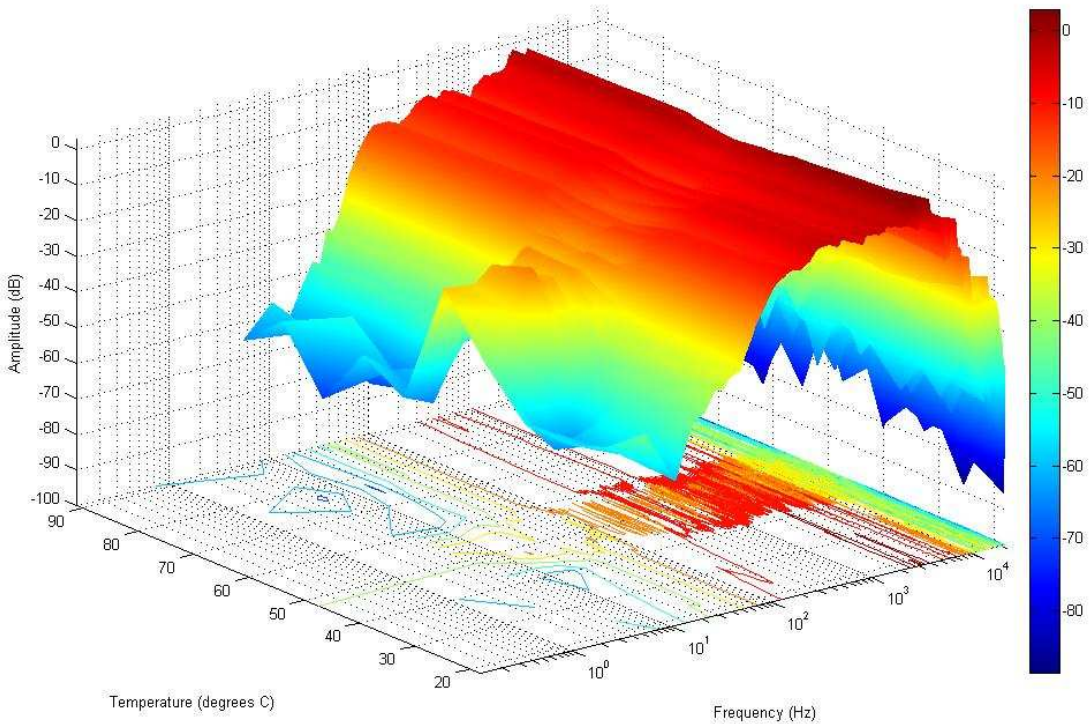

Figure 6.44: Frequency response vs. temperature plot with data errors

An additional source of error might be fluctuations in amplifier performance as the amplifier heats up over time. This wasn't overly apparent, but may have slightly affected the data after long periods of heavy use.

8. Conclusion

Through research, simulation and experimentation, it is clear that voice coil temperature affects the performance of a loudspeaker. The majority of these effects occur due to the direct relationship between the voice coil temperature and DC resistance. The change in DC resistance can affect the majority of performance parameters including electrical impedance, efficiency and axial SPL. The increase in DC resistance also causes certain low frequency values (around 110 Hz in the tested loudspeaker) to increase in amplitude as temperature rises. This can be attributed to the changes in the electrical impedance and quality factor around the nearby resonant frequency (90 Hz in this case).

Aside from the DC resistance relationship, the voice coil temperature also causes the enclosed air in a loudspeaker to rise in temperature. This will bring a rise in the speed of sound inside the enclosure, causing the response pattern to shift upwards with temperature.

While the low frequency range is largely unaffected by the voice coil temperature, high frequencies experience a significant decrease in amplitude. This is likely due to the change in stiffness of the enclosed air making it harder for the driver to move at high velocities without any lag.

The most interesting frequency range affected by voice coil temperature is a mid-range band. The explanation presented in this paper is that this drop in amplitude is due to the resonant modes due to the enclosure dimensions. These modes interact to cause significant drops in this frequency range that become more visible as the voice coil temperature rises.

All these effects on the frequency response were present at all measurement positions ranging from perfectly on-axis to ninety degrees off-axis. The only differences in response between these positions were due to phase related issues and had no dependence on the voice coil temperature.

Future work concerning this subject should include experimentation with different driver and enclosure combinations and also experimentation with the driver suspended in free-air. When in free air will the mid-range loss in response be present or is this drop indeed due to the enclosure dimensions? Also, does the amount of insulation inside the enclosure affect the

magnitude of this drop? These questions must be answered before the mid-range drop in response can be clearly explained.

It is clear that the simulated and measured frequency response changes due to the voice coil temperature are legitimate consequences thanks to repeated tests giving identical results. This drop in response is easily noticeable in a situation where the loudspeaker has been under heavy drive for an extended period of time. The high frequency loss will make for a muddier sound with the boost around 110 Hz (for this tested loudspeaker) adding to this effect. Also, peak SPL will be considerably lower at higher temperatures.

Voice coil temperature rise is an issue that cannot be ignored in loudspeaker design. Efficient heat transfer mechanisms must be present in the design. Also, the great temperature increase must be considered when choosing construction materials. The driver must be able to remain consistently functional throughout this large temperature range to be a successful driver design. Even with these considerations, though, a loudspeaker will most certainly experience a decrease in performance do to the rise in voice coil temperature.

9. List of References

[1] Eargle, John. “Loudspeaker Handbook – Second Edition.” Kluwer Academic Publishers. New York, USA. 2003.

[2] Davis, Don. “Sound System Engineering – Third Edition.” Focal Press. New York, USA. 2006.

[3] Kemp, Jonathan A. “Theoretical and experimental study of wave propagation in brass musical instruments.” University of Edinburgh. Edinburgh, UK. 2002.

[4] Hsu, Kenneth. “Simulation of Room Acoustics.” University of Queensland, Australia. November, 1996.

[5] Hsu, T.S. “Temperature prediction of the voice coil of a moving coil loudspeaker by computer simulation.” National University of Singapore. January, 1999.

[6] Anderson, Ronny. “Loudspeaker voice coil temperature estimation.” Lulea University of Technology. March 8, 2008.

[7] Bjor, Ole Herman. “Maximum Length Sequence.” Norsonic. Tranby , Norway. 2000.

[8] Gander, Mark R. “Dynamic linearity and power compression in moving-coil loudspeakers.” JBL, Inc. Northridge, California, USA. September, 1986.

[9] Hendricksen, Cliff. “Heat transfer mechanisms in loving-coil loudspeakers.” Altec Corporation. Anaheim, California, USA. 1977.

[10] Picinali, Lorenzo. “Techniques for the extraction of the impulse response of a linear and time-invariant system.” De Montfort University. Leicester, UK. 2006.

[11] Small, Richard H. “Closed-box loudspeaker systems. Part I: Analysis.” University of Sydney, Australia. December, 1972.

[12] Hawksford, M. O. J. “Distortion reduction in moving-coil loudspeaker systems using current drive technology.” University of Essex. Colchester, UK. March, 1989.

[13] Hawksford, M. O. J. “Transconductance Power Amplifier Systems for Current-Driven Loudspeakers.” University of Essex. Colchester, UK. October, 1989.

[14] Fane International Ltd. “Sovereign 8-125 Specifications.” http://www.fane-acoustics.com/pdfs/Sovereign8-125_SpecSheet.pdf

[15] Kemp, Jonathan A. “Improvements to Bore Profile Measurement in Acoustic Pulse Reflectometry.” Proceedings of the Institute of Acoustics. Volume 30, Part 2. 2008.

[16] Kinsler, Lawrence E. “Fundamentals of Acoustics – Fourth Edition.” John Wiley & Sons, Inc. New York, USA. 2000.

[17] Dedieu, Stephane. “Loudspeaker enclosure incorporating a leak to compensate for the effect of acoustic modes on loudspeaker frequency response.” Mitel Networks Corp (CA) EP1542496. 2005. http://www.freepatentsonline.com/EP1542496A1.html.

[18] Schoenherr, Steven E. “Loudspeaker History.” University of San Diego. 2001. http://history.sandiego.edu/GEN/recording/loudspeaker.html

Appendix A – MATLAB software user's guide

This section serves as a simple guide to help in successful operation of the final versions of the MATLAB simulation, measurement and analysis software developed for this project.

Simulation software

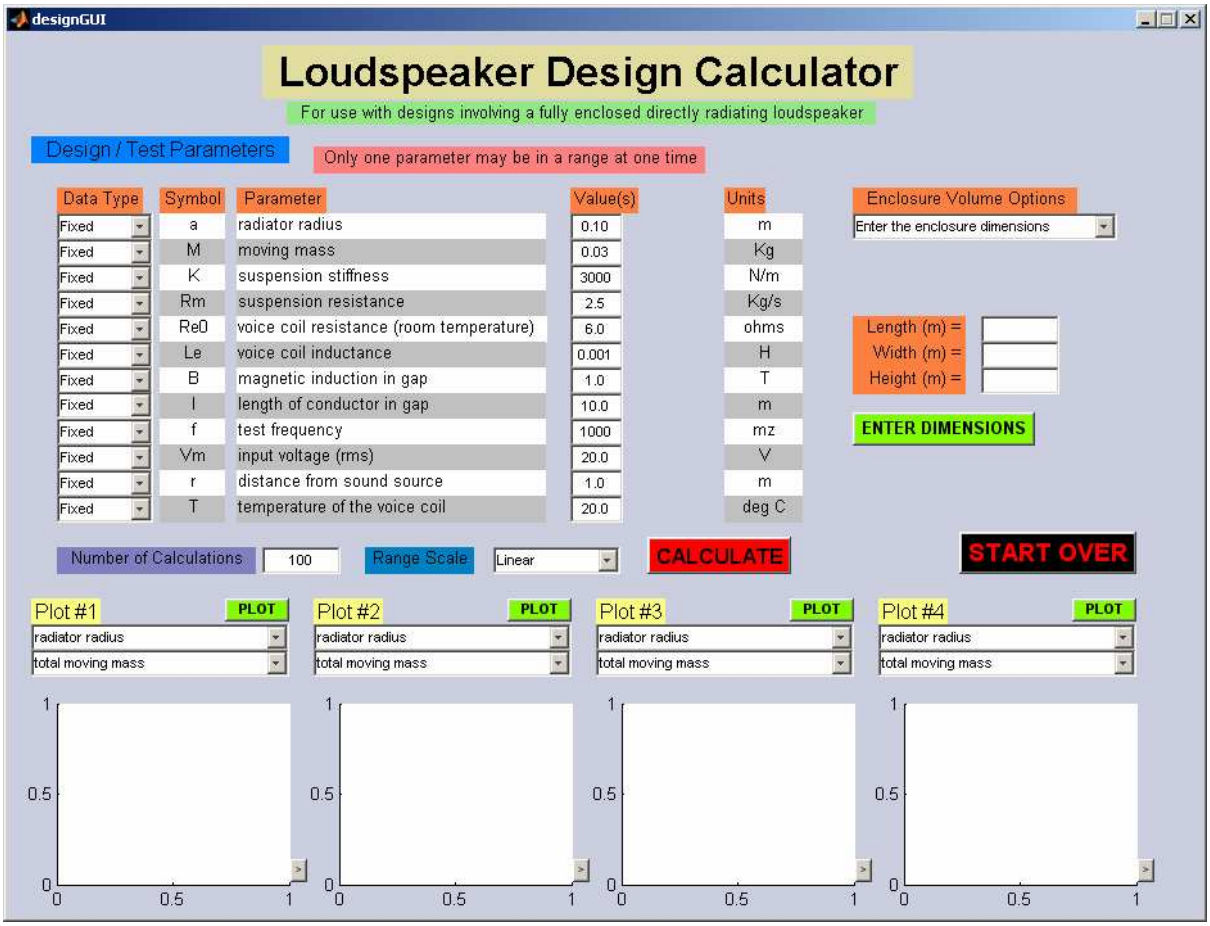

1. Switch MATLAB directory to ~/…/FINAL SOFTWARE / SIMULATION/
2. Type "designGUI" in the MATLAB command prompt. Press enter
3. Chose the appropriate method for determining the enclosure volume:
   i. Calculate the ideal volume for maximally flat response
   ii. Enter the measured enclosure volume. Press "ENTER DIMENSIONS"
   iii. Enter the measured enclosure dimensions. Press "ENTER DIMENSIONS"
4. Enter the loudspeaker's Thiele-Small parameters
5. Choose a parameter to sweep (only one). Enter the sweep range.
6. Choose a linear of logarithmic x-axis scale for plotting and number of points
7. Press "CALCULATE"
8. Choose the relationships to plot. Press appropriate "PLOT" button
9. Press the ">" buttons to expand the plotting window
10. Press "START OVER" to clear the plots to start again

Measurement software

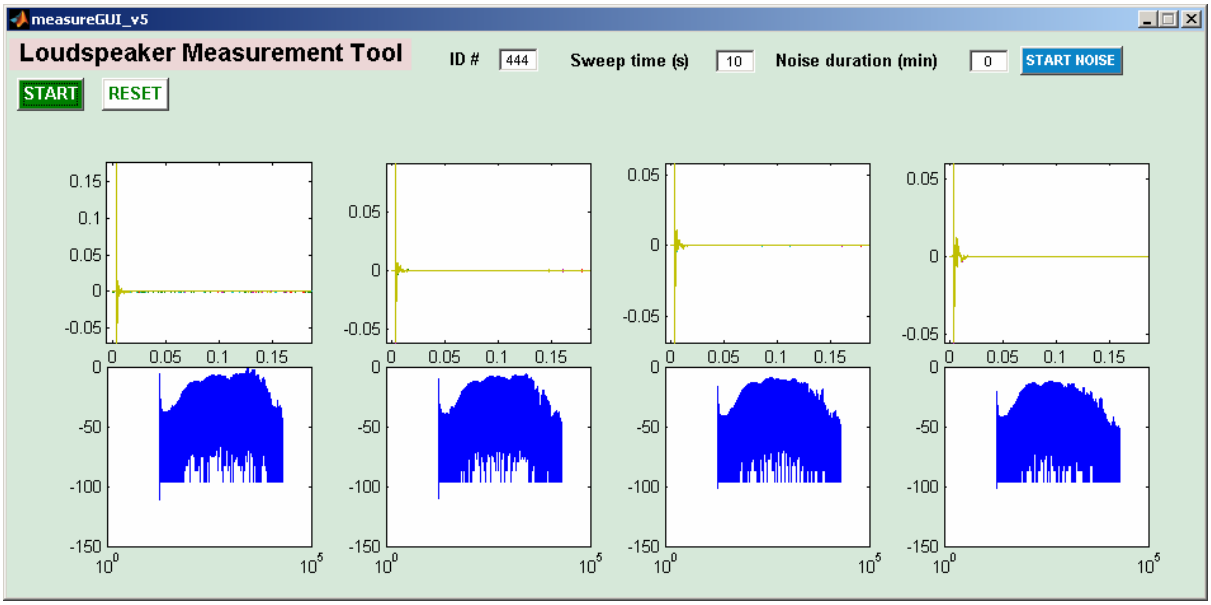

1. Switch MATLAB directory to ~/…/FINAL SOFTWARE/MEASUREMENT/
2. Type “measurementGUI_v5” in the MATLAB command prompt. Press enter
3. Define the measurement ID number
4. Define the logarithmic sweep time (in seconds)
5. Define the white noise duration (in minutes) between measurements
6. Press “START”
7. Place the loudspeaker at 0° (on-axis), when prompted, and press enter
8. Rotate the loudspeaker to 30° off-axis, when prompted, and press enter
9. Rotate the loudspeaker to 60° off-axis, when prompted, and press enter
10. Rotate the loudspeaker to 90° off-axis, when prompted, and press enter
11. If necessary, note the measured temperature and DC resistance
12. Choose whether to save the data to .wav files, when prompted
13. Choose whether to take another measurement, when prompted
14. DO NOT PUSH ANY KEYBOARD BUTTONS
15. Press “START NOISE,” wait for noise to complete and go back to step 7

NOTE: After the “START” button has been pressed, DO NOT press any more keyboard buttons UNLESS the loudspeaker is in proper position and are prompted to press enter. Pressing any keys at any other times will cause the measurements to be taken at improper times.

Analysis software

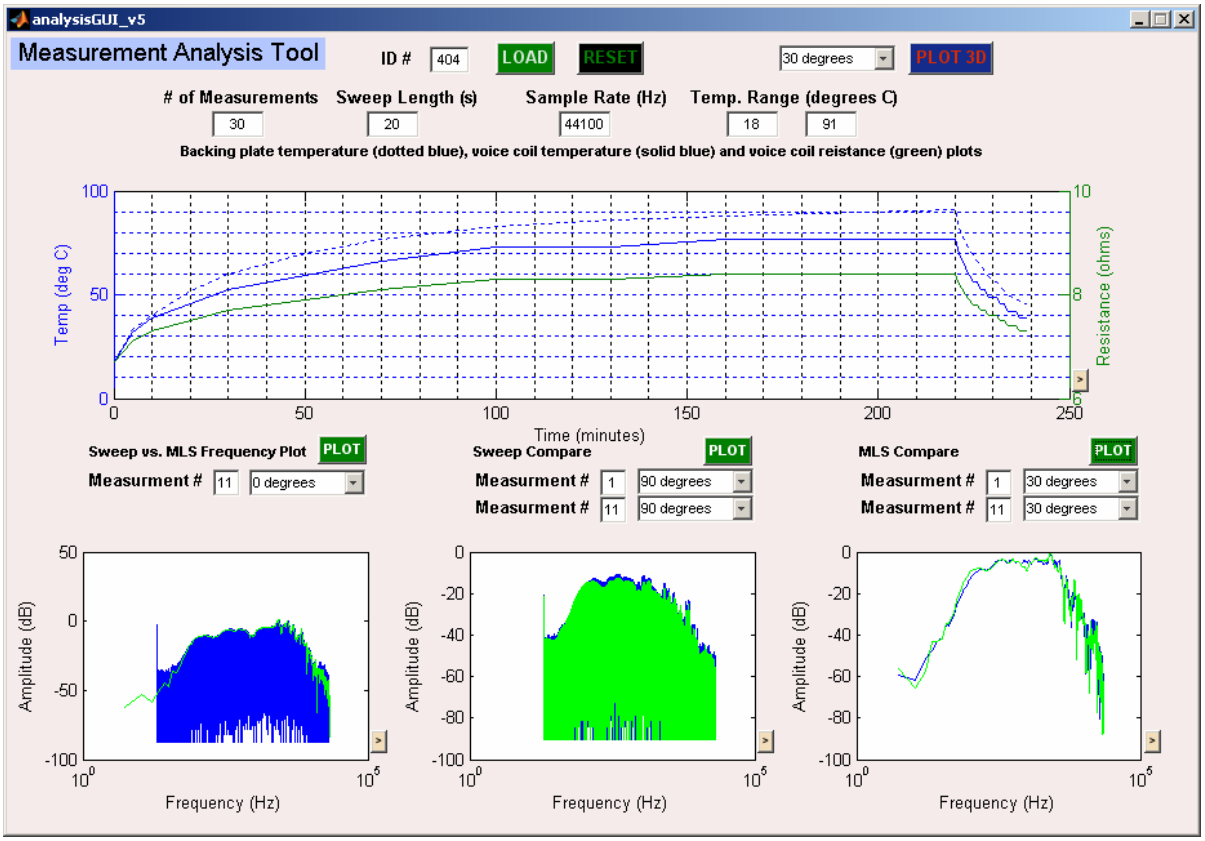

1. Switch MATLAB directory to ~/…/FINAL SOFTWARE/MEASUREMENT/
2. If necessary, locate .wav files from previous measurements
   a. Take all measurements with the same ID number and place them in a folder titled with the ID number
   b. Open getData_v2.m
      i. Add the proper case number
      ii. Enter the number of measurements taken (num)
      iii. Enter the duration of the sweep (dur)
      iv. Enter a vector of the time gap between measurements (gap)
      v. Enter the sample rate (Fs)
      vi. Enter a vector of measured temperatures (T)
      vii. Enter a vector of measured DC voice coil resistances (Re)
   c. Save and close getData_v2.m
3. If no new measurements have been taken the following ID numbers are already available for immediate analysis: 401, 402, 403, 404
4. Type “analysisGUI_v5” in the MATLAB command prompt. Press enter
5. Enter the appropriate ID number and click load
6. Choose which measurements to plot and press proper “PLOT” button
7. For a spectrogram, click “PLOT 3D” (may take a while)
8. Click any “>” button to expand any plotting window
9. Click “RESET” to start over